UNIVERSIDAD SAN FRANCISCO DE QUITO USFQ

Colegio de Ciencias e Ingenierías

Anisotropic interior solutions and gravitational decoupling

Julio César Andrade Landeta

Director de tesis: Ernesto Contreras

Física

Trabajo de titulación presentado como requisito
para la obtención del título de Magister en Física

Quito, January 18, 2022

UNIVERSIDAD SAN FRANCISCO DE QUITO USFQ

Colegio de Ciencias e Ingenierías

Hoja de calificación de trabajo de titulación

Anisotropic interior solutions and gravitational decoupling

Julio César Andrade Landeta

Nombre del director de tesis, Título académico: Ernesto Contreras, Ph.D.

Calificación: _____

Firma: _____

Quito, January 18, 2022

©DERECHOS DE AUTOR

Nombre del estudiante: Julio César Andrade Landeta

Código del estudiante: 00215908

C.I.:   1003226378

Lugar y fecha: Quito, January 18, 2022

ACLARACIÓN PARA PUBLICACIÓN

UNPUBLISHED DOCUMENT

DEDICATION

This work is dedicated to my mother.

ACKNOWLEDGEMENTS

First I want to thank the Universidad San Francisco de Quito since the achievement of this work became a reality thanks to the scholarship program of the Colegio de Ciencias e Ingenierías.

Likewise, I would like to thank Darío Niebieskikwiat who has always been attentive to my study process in the Master's degree.

To all my professors that I had the pleasure of meeting during this Master's trip for sharing their knowledge and fostering high-level academic human resources in the area of scientific research.

To my colleagues for offering me their friendship and maintaining close ties of collaboration. In a very special way I must express my gratitude to Ernesto Contreras for instilling in me the spirit of strong work in academic research, his continuous guidance, mentoring and motivation during the realization of this project.

Resumen

En este trabajo se construye modelos estelares basados en el factor de complejidad para sistemas autogravitantes estáticos y esféricamente simétricos como condición suplementaria para cerrar el sistema de ecuaciones que surgen del Desacoplamiento gravitacional. La complejidad usada es una generalización de la conocida solución Tolman IV. Se usan las soluciones Tolman IV, Wyman IIa, Durgapal IV y Heintzmann IIa como soluciones semillas. Para el análisis de la aceptabilidad física de los modelos se utiliza los parámetros de compacticidad correspondientes a los sistemas SMC X-1 y Cen X-3. Además, se usa el concepto de cracking para analizar la respuesta de estos modelos bajo la presencia de pequeñas perturbaciones justo después de abandonar el estado de equilibrio.

Palabras clave: Complejidad, desacoplamiento, semilla, sistemas, equilibrio.

Abstract

In this work, stellar models based on the complexity factor for static and spherically symmetric self-gravitating systems are constructed as a supplementary condition to close the system of equations arising from gravitational decoupling. The complexity used is a generalization of the well-known Tolman IV solution. Tolman IV, Wyman IIa, Durgapal IV and Heintzmann IIa solutions are used as seed solutions. For the analysis of the physical acceptability of the models, the compactness parameters corresponding to the SMC X-1 and Cen X-3 systems are used. Furthermore, the concept of cracking is used to analyze the response of these models under the presence of small disturbances just after leaving the steady state.

Keywords: Complexity, decoupling, seed, systems, equilibrium.

Table of contents

List of Tables

List of Figures

Chapter 1

Introduction

At the end of the year 1915 Albert Einstein published his field equations of General Relativity (GR) [1, 2], which describe the gravitational interaction in terms of the deformation of curved space-time due to the presence of matter and energy in the Universe [3]. In 1916 Karl Schwarzschild [4] found the first exact solution of Einstein's field equations, which describes the gravitational field generated by a static self-gravitating object and spherically symmetric [5,6]. Since then, questions have arisen as to whether gravitational structures with spherical symmetry that have variations in their density can be explored and if so, what kind of these variations are physically permissible.

After more than a century, various solutions have been developed for Einstein's field equations [7–9], both exact and numerical. It is worth highlighting the pioneering work carried out by Richard C. Tolman [10] for static fluid spheres where a set of five new isotropic analytical solutions are provided, which lead to subsequent studies of stellar structures such as neutron stars or star clusters through the use of GR [11]. Tolman himself raises, in his work, the im-

portance of carrying out more extensive studies in terms of finding solutions that are not purely static and analyzing the stability and plausibility of such solutions.

In 1998, Delgaty and Lake [12] found that out of the 127 isotropic solutions found in the literature at that time, 16 passed the physical acceptability tests [13, 14]. In addition, it is known that in various situations the isotropic interior hypothesis loses validity since the anisotropy in relativistic physical structures can be diverse, such as high densities, the presence of viscosity, internal magnetic fields, the presence of solid nuclei inside these structures, phase transitions, pion condensates, gas mixtures or other phenomena [15, 16]. Likewise, Hillebrandt et.al. [17] showed that the effects produced by anisotropy cannot be neglected in order to describe bodies such as neutron stars. Recently L. Herrera [18] has proven that the existence of dissipative flows, and/or inhomogeneities of energy density and/or the appearance of shear stresses in the flow of the isotropic fluid produce instability. Such instability causes that the fluid acquire the tendency to acquire the anisotropy pressure regime under conditions expected in stellar evolution. The study of anisotropic solutions started with Bowers and Liang [19] and Florides [20] followed by the work of M. Consenza et al. [21] who presented a heuristic method for obtaining models of anisotropic spheres in GR. Some recent work has been put into developing algorithms to find all anisotropic solutions and symmetrically spherical static polytropes of anisotropic fluids [22–24].

Recently, a new technique has been developed to find anisotropic solutions in a direct and efficient way by J.Ovalle [25] called Gravitational Decoupling through Minimal Geometric Deformation (MGD), which allows to extend physically acceptable isotropic solutions into the anisotropic domain while preserving the original physical acceptability [26, 27]. This technique

was extended to a more recent version known as Gravitational Decoupling through Extended Minimal Geometric Deformation (MGDe) [28] in order to study the consequences of the modified GR [29, 30], dark matter conjectures [31, 32], and the study of black holes [33, 34].

The MGD allows reducing the number of degrees of freedom in Einstein's field equations, but, nevertheless, arbitrariness remains, which can be completed with some equation of state or some metric condition. In this work we shall use a recent quantity called complexity factor for static self-gravitating symmetric spheres. Such quantity is a scalar that appears in the orthogonal splitting of the Riemman Tensor developed by Bel [35], and was used by L. Herrera [36] to define complexity for self–gravitating fluids, which is based on the idea that the least complex gravitational system is the one supported by a homogeneous energy density distribution and isotropic pressure. Assuming this complexity factor, it is possible to close the system because it provides an equation of state.

Additionally, the stability of self-gravitating compact objects has also been extensively studied since the seminal works of Bondi [37] and Chandrasekhar [38–40]. In such sense Bondi proposed a physical intuitive criterium of adiabatic stability while Chandrasekhar developed a more detailed formalism, widely used in GR. Later in 1992, L. Herrera [41] introduced the concept of "cracking" for self-gravitating compact objects proposing an alternative approach to observe the behaviour of such systems just after they depart from equilibrium [42, 43].

In this work, the construction process of new static and spherically symmetric anisotropic stellar models in the framework of the Gravitational Decoupling is shown. Such solutions are based on the generalized complexity factor of Tolman IV solution as auxiliary condition to

solve the system of differential equations arising from the MGD. Also an study of their stability against perturbation is presented. This work is organized as follows. The next chapter is devoted to review the whole theoretical framework necessary to our purposes mentioned before; the Einstein's field equations, general aspects of interior solutions, specific solutions, anisotropic solutions, basics conditions of physical acceptability, Gravitational Decoupling and Cracking of compact objects. In chapter 3 we calculate and generalize the complexity factor of the Tolman IV solution and implement this result via Gravitational Decoupling to construct extension to Tolman IV, Wyman IIa, Durgapal IV and Heintzmann IIa. Also in the same chapter the perturbed total radial force for each model is constructed in order to analyze this response against small fluctuations over the matter sector. Finally, chapter 4 is devoted to interpret and discuss our results, and in the last chapter we summarize the work and supply some final comments and conclusions.

Chapter 2

Theoretical framework

2.1 Einstein's field equations

Einstein's field equations (EFE) describe the gravitation as a manifestation of curvature of space-time[1] due the presence of sources of energy and momentum. These equations respect the covariance principle of Physics, namely, they are the same by any choice of reference system, and are given by

$$G_{\mu\nu} = k^2 T_{\mu\nu} \quad \mu, \nu \in \{0, 1, 2, 3\}, \tag{2.1}$$

where $k^2 = \frac{8\pi G}{c^4}$[2]. In the left hand of EFE there is the geometric information of curvature of space-time encoded in the Einstein's tensor $G_{\mu\nu}$

$$G_{\mu\nu} = R_{\mu\nu} - \frac{1}{2} R g_{\mu\nu}, \tag{2.2}$$

---

[1]Mathematically the space-time in GR is a continuous and differential manifold of four dimensions whose coordinates are x^μ such that $\mu \in \{0, 1, 2, 3\}$: one temporal dimension (x^0) and three spacial dimensions (x^1, x^2, x^3).

[2]c is the vacuum speed of light and G is the universal constant of gravitation.

where $R_{\mu\nu}$ and R are the Ricci's tensor and Ricci's scalar defined by contractions of Riemman's tensor $R^{\lambda}_{\mu\rho\nu}$ as

$$R_{\mu\nu} = g^{\lambda\rho}R_{\lambda\mu\rho\nu} = R^{\rho}_{\mu\rho\nu} \tag{2.3}$$

$$R = g^{\mu\nu}R_{\mu\nu}, \tag{2.4}$$

with $g_{\mu\nu}$ the metric tensor.

The Riemman's tensor is defined through the connections $\Gamma^{\sigma}_{\mu\nu}$ and their derivatives

$$R^{\sigma}_{\mu\rho\nu} = \partial_\rho\Gamma^{\sigma}_{\mu\nu} - \partial_\nu\Gamma^{\sigma}_{\mu\rho} + \Gamma^{\sigma}_{\lambda\rho}\Gamma^{\lambda}_{\mu\nu} - \Gamma^{\sigma}_{\lambda\nu}\Gamma^{\lambda}_{\mu\rho}, \tag{2.5}$$

which are defined as

$$\Gamma^{\sigma}_{\mu\nu} = \frac{1}{2}g^{\sigma\rho}\left(\partial_\nu g_{\mu\rho} + \partial_\mu g_{\nu\rho} - \partial_\rho g_{\mu\nu}\right), \tag{2.6}$$

The right hand side of EFE contains the energy-momentum tensor $T_{\mu\nu}$, that encodes the information about all sources of energy and momentum which deform the space-time and is covariantly conserved, namely

$$\nabla_\mu T^{\mu\nu} = 0. \tag{2.7}$$

As $G_{\mu\nu}$ and $T_{\mu\nu}$ are symmetric, the EFE correspond to 10 highly non-linear differential equations for $g_{\mu\nu}$ with ten unknown quantities to be determinate: six components of $g_{\mu\nu}$ and the four non-vanishing components of $T_{\mu\nu}$ [44].

2.2 Interior solutions

In this work we model stars in the framework of GR as self-gravitating fluid compact objects with spherical symmetric configuration in hydrostatic equilibrium surrounded by empty space. Fuerthermore, due to most of the stars having long phases of stellar evolution, their structure remains unaltered by large periods of time so we shall consider them as static configurations [45, 46]. Based on the previous assumptions, we consider a line element given by

$$ds^2 = e^{\nu(r)}dt^2 - e^{\lambda(r)}dr^2 - r^2 d\theta^2 - r^2 \cos(\theta)d\phi^2, \tag{2.8}$$

where $\nu(r)$ and $\lambda(r)$ are strictly functions of the radial coordinate r.

The covariant components of the metric field $g_{\mu\nu}$ are

$$g_{00} = e^{\nu} \quad g_{11} = -e^{\lambda} \quad g_{22} = -r^2 \quad g_{33} = -r^2 \sin^2\theta, \tag{2.9}$$

so that

$$g^{00} = e^{-\nu} \quad g^{11} = -e^{-\lambda} \quad g^{22} = -\frac{1}{r^2} \quad g^{33} = -\frac{1}{r^2 \sin^2\theta}. \tag{2.10}$$

From now on we shall assume $c = G = 1$ so that $k^2 = 8\pi$. Now, the only non vanishing components of Einstein's tensor $G_{\mu\nu}$ associated with the metric in Eq. (2.8) are (See Appendix A for details)

$$G_{00} = -\frac{e^{-(\lambda-\nu)}}{r^2}(1 - \lambda'r - e^{\lambda}) \tag{2.11}$$

$$G_{11} = \frac{1}{r^2}(1 - e^{\lambda} + \nu'r) \tag{2.12}$$

$$G_{22} = r^2 e^{-\lambda} \left(\frac{\nu''}{2} - \frac{\lambda'\nu'}{4} + \frac{(\nu')^2}{4} + \frac{\nu' - \lambda'}{2r} \right) \tag{2.13}$$

$$G_{33} = G_{22} \sin^2 \theta, \tag{2.14}$$

where the differentiation with respect to radial coordinate r for any function f is indicated by $f' \equiv \partial_r f$.

At first approximation the interior of star can be considered as a relativistic perfect fluid, in such a way that the associated energy-momentum tensor $T_{\mu\nu}$ can be written

$$T_{\mu\nu} = (\rho + p)u^\mu u^\nu - pg^{\mu\nu}, \tag{2.15}$$

where ρ, p and u^μ are the energy density, pressure and the four-velocity of the fluid, respectively. So considering $u^\mu u_\mu = 1$ for a local inertial observer at rest with the fluid results in $u^\mu = (e^{-\nu/2}, 0, 0, 0)$ and

$$T^\mu_\nu = diag(\rho, -p, -p, -p) = \begin{pmatrix} \rho & 0 & 0 & 0 \\ 0 & -p & 0 & 0 \\ 0 & 0 & -p & 0 \\ 0 & 0 & 0 & -p \end{pmatrix}. \tag{2.16}$$

Then, using Eqs. (2.11)-(2.14) and (2.16) in Eq. (2.1) we arrive at

$$8\pi\rho = \frac{1}{r^2} + e^{-\lambda}\left(\frac{\lambda'}{r} - \frac{1}{r^2}\right) \tag{2.17}$$

$$8\pi p = -\frac{1}{r^2} + e^{-\lambda}\left(\frac{\nu'}{r} + \frac{1}{r^2}\right) \tag{2.18}$$

$$8\pi p = \frac{e^{-\lambda}}{4}\left(2\nu'' - \lambda'\nu' + \nu'^2 + 2\frac{\nu' - \lambda'}{r}\right), \tag{2.19}$$

which are the Einstein's field equations for a perfect fluid distribution.

The above system of equations consists of three nonlinear coupled differential equations with four unknown quantities ρ, p, ν and λ so an extra condition is required.

The conservation of the energy-momentum tensor leads to

$$\frac{dp}{dr} = -\frac{1}{2}\nu'(\rho + p), \tag{2.20}$$

which is known as the Tolman–Oppenheimer–Volkoff equation (TOV) for an isotropic fluid in hydrostatic equilibrium. The TOV equation can be interpreted as an equation of balance between forces, where the hydrostatic force $F_h = \frac{dp_r}{dr}$ is balanced by the gravitational force $F_g = \frac{1}{2}\nu'(\rho + p_r)$. Introducing the mass function mass $m(r)$ the g^{rr} component of the metric can be written as

$$e^{-\lambda} \equiv 1 - \frac{2m(r)}{r}. \tag{2.21}$$

Now from (2.17) and (2.18) we obtain

$$\frac{1}{2}\nu' = \frac{m + 4\pi r^3 p}{r(r - 2m)},$$ (2.22)

so that the TOV can be expressed as

$$\frac{dp}{dr} = -\frac{(\rho + p)(m + 4\pi r^3 p)}{r(r - 2m)}.$$ (2.23)

Note that since in this work we will refer only to stars composed of non-exotic matter then $\rho > 0$, it implies that $\frac{dp}{dr} < 0$, namely, p is an decreasing function of r.

2.3 Exact isotropic specific solutions

A way to obtain exact solutions for the set of equations (2.17)-(2.19) was developed in 1939 by Tolman [10], which consists of writing these equations as:

$$0 = \frac{d}{dr}\left(\frac{e^{-\lambda} - 1}{r^2}\right) + \frac{d}{dr}\left(\frac{e^{-\lambda}\nu'}{2r}\right) + e^{-\lambda-\nu}\frac{d}{dr}\left(\frac{e^{\nu}\nu'}{2r}\right)$$ (2.24)

$$8\pi p = e^{-\lambda}\left(\frac{\nu'}{r} + \frac{1}{r^2}\right) - \frac{1}{r^2}$$ (2.25)

$$8\pi\rho = e^{-\lambda}\left(\frac{\lambda'}{r} - \frac{1}{r^2}\right) + \frac{1}{r^2},$$ (2.26)

then, imposing certain conditions for the components of the metric as is indicated in what follows.

2.3.1 Einstein's universe solution

In this case its assumed that e^ν is an arbitrary constant, namely, $e^\nu = constant = k$, so that $\nu' = 0$ and the system of Eqs. (2.24)-(2.26) in this case becomes

$$0 = \frac{d}{dr}\left(\frac{e^{-\lambda} - 1}{r^2}\right) \tag{2.27}$$

$$8\pi p = \frac{e^{-\lambda}}{r^2} - \frac{1}{r^2} \tag{2.28}$$

$$8\pi\rho = e^{-\lambda}\left(\frac{\lambda'}{r} - \frac{1}{r^2}\right) + \frac{1}{r^2}. \tag{2.29}$$

From the integration of Eq. (2.27) we obtain

$$e^\lambda = \frac{1}{1 - \frac{r^2}{C^2}}, \tag{2.30}$$

where C is integration constant. Then using Eq. (2.30) in (2.28) p is obtained, that is

$$8\pi p = -\frac{1}{C^2}, \tag{2.31}$$

and from Eq. (2.29)

$$8\pi\rho = \frac{3}{C^2}. \tag{2.32}$$

The previous results can be summarized as

$$e^\nu = constant = k \tag{2.33}$$

$$e^\lambda = \frac{1}{1 - \frac{r^2}{C^2}} \tag{2.34}$$

$$8\pi\rho = \frac{3}{C^2} \tag{2.35}$$

$$8\pi p = -\frac{1}{C^2}. \tag{2.36}$$

Note that

$$\rho = -3p. \tag{2.37}$$

2.3.2 Schwarzschild-de Sitter solution

In this case is assumed that $e^{-\lambda-\nu} = constant$, so that (2.24) gives

$$e^{-\lambda}\left(\frac{1}{r^2} + \frac{\nu'}{r}\right) - \frac{1}{r^2} = C, \tag{2.38}$$

where C is an integration constant. Now, since $e^{-\lambda-\nu} = constant$, it follows that $\lambda' = -\nu'$, then

$$e^{-\lambda}\left(\frac{\lambda'}{r} - \frac{1}{r^2}\right) + \frac{1}{r^2} = -C. \tag{2.39}$$

Thus, from Eqs. (2.38) and (2.39) in Eqs. (2.28)-(2.29) one obtains

$$e^\nu = \left(1 - \frac{2m}{r} - \frac{r^2}{C^2}\right) \tag{2.40}$$

$$e^\lambda = \left(1 - \frac{2m}{r} - \frac{r^2}{C^2}\right)^{-1} \tag{2.41}$$

$$8\pi\rho = -C \tag{2.42}$$

$$8\pi p = C, \tag{2.43}$$

which is well known as Schwarzschild-de Sitter solution for a de Sitter universe with a spherically symmetrical body at the origin of coordinates. If $C \longrightarrow \infty$ the solution becomes

$$e^\nu = 1 - \frac{2m}{r} \tag{2.44}$$

$$e^\lambda = \left(1 - \frac{2m}{r}\right)^{-1}, \tag{2.45}$$

which is the well known Schwarzschild exterior solution. If $m = 0$ it turns into the usual form for the de Sitter universe.

2.3.3 Schwarszchild interior solution

In this case we assumed that $e^{-\lambda} = 1 - \frac{r^2}{C^2}$ with C being a constant, from where (2.24) becomes

$$\frac{d}{dr}\left(\frac{e^{-\lambda}\nu'}{2r}\right) + e^{-\lambda-\nu}\frac{d}{dr}\left(\frac{e^\nu\nu'}{2r}\right) = 0. \tag{2.46}$$

Now, if the previous equation is multiplied by $\frac{e^\nu\nu'}{2r}$ it is found that

$$e^{\frac{\nu}{2}}d\nu = \frac{2Brdr}{\sqrt{1-\frac{r^2}{C^2}}} \tag{2.47}$$

where B is a integration constant. Performing an additional integration we have

$$e^{\nu} = \left[A - B \left(1 - \frac{r^2}{C^2} \right)^{1/2} \right]^2 . \qquad (2.48)$$

where A is another integration constant. Now, using $e^{-\lambda} = 1 - \frac{r^2}{C^2}$, Eq. (2.26) leads to

$$8\pi\rho = \frac{3}{C^2} . \qquad (2.49)$$

Replacing $e^{-\lambda}$ and Eq. (2.48) in Eq. (2.25) we obtain

$$8\pi p = \frac{1}{C^2} \left(\frac{3B \left(1 - \frac{r^2}{C^2} \right) - A}{A - B \left(1 - \frac{r^2}{C^2} \right)^{1/2}} \right) . \qquad (2.50)$$

In summary, the Schwarszchild interior solution is

$$e^{-\lambda} = 1 - \frac{r^2}{C^2} \qquad (2.51)$$

$$e^{\nu} = \left[A - B \left(1 - \frac{r^2}{C^2} \right)^{1/2} \right]^2 \qquad (2.52)$$

$$\rho = \frac{3}{8\pi C^2} \qquad (2.53)$$

$$p = \frac{1}{8\pi C^2} \left(\frac{3B \left(1 - \frac{r^2}{C^2} \right)^{1/2} - A}{A - B \left(1 - \frac{r^2}{C^2} \right)^{1/2}} \right) . \qquad (2.54)$$

Note that if we impose $B = 0$, the system of Eqs. (2.51)-(2.54) turns into the Einstein's universe solution and if $A = 0$, the de Sitter universe is found.

2.3.4   Tolman IV solution

For this case we assume that $\frac{e^\nu \nu'}{2r} = constant = k$, which implies that $e^\nu = kr^2 + k'($ with k' another constant). Now, if we define $k = \frac{B^2}{A^2}$ and $k' = B^2$, we obtain

$$e^\nu = B^2 \left(\frac{r^2}{A^2} + 1 \right). \tag{2.55}$$

Using the above metric component in Eq. (2.24) results in

$$e^\lambda = \frac{1 + \frac{2r^2}{A^2}}{(1 + \frac{r^2}{A^2})(Kr^2 + 1)}, \tag{2.56}$$

where K is an integration constant. Now, it is convenient to choose $K = -\frac{1}{C^2}$, from where

$$e^\lambda = \frac{1 + \frac{2r^2}{A^2}}{(1 + \frac{r^2}{A^2})(1 - \frac{r^2}{C^2})}. \tag{2.57}$$

After using Eqs. (2.55) and (2.57) in Eqs. (2.25) and (2.26), we obtain

$$8\pi\rho = \frac{2}{A^2} \frac{1 - \frac{r^2}{C^2}}{\left(1 + \frac{2r^2}{A^2}\right)^2} + \frac{1 + \frac{3A^2}{C^2} + \frac{3r^2}{C^2}}{A^2 \left(1 + \frac{2r^2}{A^2}\right)} \tag{2.58}$$

$$8\pi p = \frac{1 - \frac{A^2}{C^2} - \frac{3r^2}{C^2}}{A^2(1 + \frac{2r^2}{A^2})}. \tag{2.59}$$

In summary, the known Tolman IV solution is

$$e^{\nu} = B^2 \left(\frac{r^2}{A^2} + 1 \right) \tag{2.60}$$

$$e^{-\lambda} = \frac{(C^2 - r^2)(A^2 + r^2)}{C^2(A^2 + 2r^2)} \tag{2.61}$$

$$\rho = \frac{3A^4 + A^2(3C^2 + 7r^2) + 2r^2(C^2 + 3r^2)}{8\pi C^2(A^2 + 2r^2)^2} \tag{2.62}$$

$$p = \frac{C^2 - A^2 - 3r^2}{8\pi C^2(A^2 + 2r^2)}. \tag{2.63}$$

2.3.5 Wyman IIa solution

In this case we show the Wyman IIa solution [12, 47] with $n = 2$ whose metric components read

$$e^{\nu} = (A - Br^2)^2 \tag{2.64}$$

$$e^{-\lambda} = 1 + Cr^2(A - 3Br^2)^{-2/3}, \tag{2.65}$$

where A, B and C are constants.

Now using these metric components (2.64) and (2.65) in (2.17)-(2.19) we obtain

$$\rho = \frac{(5Br^2 - 3A)C}{8\pi \left(A - 3Br^2 \right)^{5/3}} \tag{2.66}$$

$$p = \frac{\left(5 - \frac{4A}{A - Br^2} \right) \left(\frac{Cr^2}{(A - 3Br^2)^{2/3}} + 1 \right) - 1}{8\pi r^2}. \tag{2.67}$$

This solution is a generalization of Tolman VI solution [10, 47]. The Wyman IIa (with $n = 2$) solution is not completely satisfactory from physical of view.

2.3.6 Durgapal IV solution

In this case we consider the Durgapal IV solution [12, 48] whose metric components read

$$e^\nu = A(Cr^2 + 1)^4 \tag{2.68}$$

$$e^{-\lambda} = \frac{7 - 10Cr^2 - C^2r^4}{7(Cr^2 + 1)^2} + \frac{BCr^2}{(Cr^2 + 1)^2(1 + 5Cr^2)^{2/5}}, \tag{2.69}$$

where A, B and C are constants. Now using (2.64) and (2.65) in (2.17)-(2.19) we obtain

$$\rho = \frac{C\left(7B\left(Cr^2\left(9Cr^2 - 10\right) - 3\right) + 8\left(Cr^2\left(Cr^2 + 2\right) + 9\right)\left(5Cr^2 + 1\right)^{7/5}\right)}{56\pi\left(Cr^2 + 1\right)^3\left(5Cr^2 + 1\right)^{7/5}} \tag{2.70}$$

$$p = \frac{C\left(7B\left(9Cr^2 + 1\right) - 16\left(5Cr^2 + 1\right)^{2/5}\left(Cr^2\left(Cr^2 + 7\right) - 2\right)\right)}{56\pi\left(Cr^2 + 1\right)^3\left(5Cr^2 + 1\right)^{2/5}}. \tag{2.71}$$

This solution is completely satisfactory from physical of view, namely, it fulfills all physical conditions detailed in the section 2.6 according to Delgaty [12].

2.3.7 Heintzmann IIa solution

In this subsection we consider the Heintzmann IIa solution [12, 49], whose metric components read

$$e^\nu = A^2\left(Br^2 + 1\right)^3 \tag{2.72}$$

$$e^{-\lambda} = 1 - \frac{3Br^2}{2}\frac{1 + C(1 + 4Br^2)^{-1/2}}{1 + Br^2}. \tag{2.73}$$

Here, A, B and C are constants, from where

$$\rho = \frac{3B\left(C\left(9Br^2+3\right)+\left(Br^2+3\right)\left(4Br^2+1\right)^{3/2}\right)}{16\pi\left(Br^2+1\right)^2\left(4Br^2+1\right)^{3/2}}, \tag{2.74}$$

$$p = -\frac{3B\left(7BCr^2+3\left(Br^2-1\right)\sqrt{4Br^2+1}+C\right)}{16\pi\left(Br^2+1\right)^2\sqrt{4Br^2+1}}. \tag{2.75}$$

Also, this solution fulfills all physical conditions detailed in the section 2.6 according to Delgaty [12].

Up to this point we have presented some well-known isotropic solutions (there are a longer number of known solutions which can be seen in [12]). It is worth mentioning that any solution must fulfill conditions explored in the following sections.

2.4   Matching conditions

Since space-time in GR is a differential and continuous geometric structure (pseudo-Riemannian manifold [50]), it should be achieved precisely on the surface Σ between the internal region of the interstellar object ($r < R$) and the external region that surrounds it ($r > R$). In this work, we will consider that the outside of the stellar distribution is empty and spherically symmetric. So, by Birkhoff theorem [51], it corresponds to the Schwarzschild exterior solution given by

$$ds^2 = \left(1-\frac{2M}{R}\right)dt^2 - \left(1-\frac{2M}{R}\right)^{-1}dr^2 - r^2d\theta^2 - r^2\sin^2\theta d\phi^2, \tag{2.76}$$

where M and R are the mass and radius of the star, respectively.

Now, Darmois [52, 53] demonstrated that the continuity of the first and the second fundamental are necessary and sufficient conditions across the surface Σ separating the interior and exterior geometries. The continuity of the first fundamental forms entails

$$\left[ds^2\right]_\Sigma = 0, \tag{2.77}$$

which in our case reads

$$\left. e^\nu \right|_{\Sigma^-} = \left. \left(1 - \frac{2M}{R}\right) \right|_{\Sigma^+} \tag{2.78}$$

$$\left. e^\lambda \right|_{\Sigma^-} = \left. \left(1 - \frac{2M}{R}\right)^{-1} \right|_{\Sigma^+}. \tag{2.79}$$

Likewise, the second fundamental form states that

$$\left[G_{\mu\nu}r^\nu\right]_\Sigma = 0, \tag{2.80}$$

where r_μ is a unit radial vector. Now, using Eq. (2.80) in (2.1), we find

$$\left[T_{\mu\nu}r^\nu\right]_\Sigma = 0, \tag{2.81}$$

from where

$$\left. p \right|_{\Sigma^-} = \left. p \right|_{\Sigma^+} = 0. \tag{2.82}$$

Up to this point we have focused on isotropic solutions, but as we will see in the next section it is necessary to extend our study to the anisotropic fluid regime in order to consider

more suitable models to describe stellar compact objects.

2.5   Spherically symmetric anisotropic solutions in GR

Despite the fact that Einstein and Lemaitre had realized that spherical symmetry only allows an equality of the tangential pressures p_t (which implies $T_{\mu\nu} = diag(\rho, -p_r, -p_t, -p_t)$ [54] where p_r is the pressure in radial direction) the stars were considered as supported by a perfect fluid for long time [13]. However, in 1972 Ruderman [55] argued for the first time that nuclear matter at very high densities in the order of $10^{15} g/cm^3$ could have anisotropy. In the same line, it was later known that anisotropy can be generated by several reasons [56] such as the mixture of different fluids, presence of superfluid, existence of solid nuclei, phase transitions, presence of magnetic fields, viscosity, etc. In this regard isotropic fluid models are not longer the most suitable for describing stars in GR.

We can start by considering a spherically symmetric static distribution of matter in equilibrium with $T_{\mu\nu} = diag(\rho, -p_r, -p_t, -p_t)$. Replacing this information in EFE (2.1) and using Eqs.(2.11)-(2.14) we obtain

$$8\pi\rho = \frac{1}{r^2} + e^{-\lambda}\left(\frac{\lambda'}{r} - \frac{1}{r^2}\right) \tag{2.83}$$

$$8\pi p_r = -\frac{1}{r^2} + e^{-\lambda}\left(\frac{\nu'}{r} + \frac{1}{r^2}\right) \tag{2.84}$$

$$8\pi p_t = \frac{e^{-\lambda}}{4}\left(2\nu'' - \lambda'\nu' + (\nu')^2 + 2\frac{\nu' - \lambda'}{r}\right). \tag{2.85}$$

Note also if $p_t = p_r = p$ one returns to EFE for isotropic case given by Eqs. (2.17)-(2.19).

Now using the condition (2.7) we obtain explicitly

$$\frac{dp_r}{dr} = -\frac{1}{2}\nu'(\rho + p_r) - \frac{2}{r}\Pi, \tag{2.86}$$

where the anisotropy function $\Pi \equiv p_r - p_t$ is defined. Equation (2.86) is known as the Tolman-Oppenheimer-Volkoff (TOV) equation for an anisotropic fluid distribution [19].

After using Eq. (2.22) (which is valid also for the anisotropic case) in Eq. (2.86), it gives us

$$\frac{dp_r}{dr} = -\frac{(\rho + p_r)(m + 4\pi r^3 p)}{r(r - 2m)} - \frac{2}{r}\Pi. \tag{2.87}$$

In the next section we shall explore the acceptability conditions for interior solutions.

2.6 Physical acceptability conditions for interior solutions

The three differential equations (2.83)-(2.85) for a spherically symmetric stellar object have five unknown quantities: the metric functions $\nu(r)$, $\lambda(r)$ and the three physical quantities ρ, p_t and p_r, which in principle can be solved if two equations of state are defined, namely, $p_r = p_r(\rho)$ and $p_t = p_t(\rho)$, or if conditions over the metric functions are given. Mathematically there are no limits to do the above. However, not all these choices would correspond to acceptable solutions from the physical point of view. Therefore, it is essential to define certain fundamental conditions that any realistic solution must satisfy [13]. In this work we consider the follow conditions:

Condition 1: Regular metric

The functions λ and ν must be positive, finite, and free of singularities inside of stellar object. Furthermore, at the center, it must be satisfied that $e^{-\lambda(0)} = 1$ and $e^{\nu(0)} = constant$.

The above is justified since

$$\lim_{r \to 0} e^{-\lambda} = 1 - \lim_{r \to 0} \frac{2m}{r} = 1 - \lim_{r \to 0} \frac{4\pi\rho(r)r^2}{r} = 1, \tag{2.88}$$

where the Eq.(2.21) was used. Now, from (2.22)

$$\lim_{r \to 0} \frac{1}{2}\nu' = \lim_{r \to 0} \frac{m(r) + 4\pi r^3 p_r}{r(r - 2m)} = 0, \tag{2.89}$$

where we have assumed that p_r and ρ are finite at the center of the star.

Condition 3: Redshift

The inner redshift z should decreases as the value of r increases. This quantity is related to the phenomenon in which photons lose energy when they travel out of a gravitational source. Such loss of energy produces a frequency of light wave decrease. So, in order to quantify this, we consider two observers at rest, one (emitter) that is on the surface of the central gravitational object at r_1, who sends a pulse of light towards the other observer (receiver) located in a very distant position at r_2. Now, due to the fact that light travels along null geodesics (null radial geodesics are considered for this analysis, $d\theta = d\phi = 0$) we have that

$$ds^2 = g_{tt}dt^2 - g_{rr}dr^2 = 0 \implies dt = \left(\frac{g_{rr}}{g_{tt}}\right)^{1/2} dr. \tag{2.90}$$

Therefore, for the two light pulses the coordinate time between two successive pulses does not change since that

$$t_2 - t_1 = \int_{r_1}^{r_2} \left(\frac{g_{rr}}{g_{tt}} \right)^{1/2} dr = constant, \tag{2.91}$$

namely $\Delta t_1 = \Delta t_2$ [57]. Since the proper time intervals $(\Delta \tau)$ are related to the coordinate time intervals Δt as $\Delta \tau = \sqrt{g_{tt}} \Delta t$, we have

$$\frac{\Delta \tau_R}{\Delta \tau_E} = \frac{\sqrt{g_{tt}^R}}{\sqrt{g_{tt}^E}}, \tag{2.92}$$

where R corresponds to the receiver and the E to the emitter. Now, as the frecuency is $\nu \sim \frac{1}{\Delta \tau}$, we arrive at

$$\frac{\nu_E}{\nu_R} = \frac{\sqrt{g_{tt}^R}}{\sqrt{g_{tt}^E}}. \tag{2.93}$$

With this, the definition of the redshift z [45] is given by

$$z = \frac{\nu_E - \nu_R}{\nu_R} = \frac{\frac{\sqrt{g_{tt}^R}}{\sqrt{g_{tt}^E}} \nu_R - \nu_R}{\nu_R} = \frac{\sqrt{g_{tt}^R}}{\sqrt{g_{tt}^E}} - 1. \tag{2.94}$$

We should emphasize that the receiver is far long from emitter, so $g_{tt}^R = 1$ and (2.94) leads to

$$z = g_{tt}^{-1/2} - 1, \tag{2.95}$$

where we have define $g_{tt}^{EE} \equiv g_{tt}$.

Condition 4: Causality

The radial $v_r^2 = \frac{dp_r}{d\rho}$ and transversal $v_t^2 = \frac{dp_t}{d\rho}$ speed of sound inside of a star do not exceed the value of light in vacuum, that is

$$0 \leq \frac{dp_r}{d\rho} < 1 \quad \text{and} \quad 0 \leq \frac{dp_t}{d\rho} < 1. \tag{2.96}$$

This condition ensures that no mechanical wave can move faster than light within the interstellar body.

Condition 5: Positive density energy and pressure

The energy density and pressure are positive inside the star. This is true since the stars that we consider in this study are composed of ordinary matter. In the stellar center these quantities must be finite $\rho(0) = \rho_0$, $p_r(0) = p_{r0}$, $p_t(0) = p_{t0}$ in order to avoid the collapse of the star [58]. In fact, at the center $p_{r0} = p_{t0}$ since $\frac{dp_r}{dr}$ must be finite at $r = 0$ (see Eq. (2.86)).

Condition 6: Matter profiles

The three physical quantities ρ, p_r and p_t must have their maximum values at stellar center and monotonously decrease outward. Explicitly this reads

$$\rho'(0) = p_r'(0) = p_t'(0) = 0, \quad \text{and} \tag{2.97}$$

$$\rho' \leq 0, p_r' \leq 0, p_t' \leq 0. \tag{2.98}$$

Now in order to prove the above it is necessary to show that the tangential pressure is greater than the radial one, except at the center. In order do so, we start from the anti-cracking condition

[13], which explicitly reads

$$-1 + \frac{dp_r}{d\rho} \leq \frac{dp_t}{d\rho} \leq \frac{dp_r}{d\rho}. \tag{2.99}$$

Now, since $0 < \frac{dp_r}{d\rho} \leq 1$ and $0 < \frac{dp_t}{d\rho} \leq 1$, the left side of the above inequality is not positive, and then

$$0 \leq \frac{dp_t}{d\rho} \leq \frac{dp_r}{d\rho}. \tag{2.100}$$

Therefore,

$$0 \leq \frac{p_t'}{\rho'} \leq \frac{p_r'}{\rho'}. \tag{2.101}$$

Now, multiplying by ρ', which is negative, we obtain

$$0 \geq p_t' \geq p_r'. \tag{2.102}$$

From where p_t y p_r are decreasing function of r, and $p_t'(0) = p_r'(0) = 0$. Then if Eq. (2.102) is integrated, we obtain that

$$0 \geq p_t - p_{t0} \geq p_r - p_{r0}, \tag{2.103}$$

and as $p_r(0) = p_t(0)$ then Eq. (2.103) becomes $p_t \geq p_r$.

Condition 7: Energy conditions

In principle, EFE can be solved for any energy-momentum tensor $T_{\mu\nu}$, but it is essential to ensure that their components belong to physically realistic sources [5]. Such conditions are expressed as inequalities on the components of the tensor $T_{\mu\nu}$ as follows [5, 59]:

1 *The Weak Energy Condition (WEC):* The energy density measured by any observer must be non-negative

$$\rho \geq 0 \tag{2.104}$$

and

$$\rho - p_r \geq 0 \quad \text{and} \quad \rho - p_t \geq 0. \tag{2.105}$$

This follows from ρ being a positive scalar for regular matter and the energy density greater than the pressures, implying the classical causality fact that matter cannot travel faster than light in vacuum.

2 *The Null Energy Condition (NEC):* The energy density may be greater than pressure since the condition of causality must be fulfilled.

$$\rho - p_r \geq 0 \quad \text{and} \quad \rho - p_t \geq 0. \tag{2.106}$$

3 *Dominant energy condition (DEC):* Radial and tangential pressures must not exceed en-

ergy density in absolute value.

$$\rho \geq |p_r| \quad \text{and} \quad \rho \geq |p_t|. \tag{2.107}$$

4 *Strong energy condition (SEC)*:

$$\rho \geq p_r, \tag{2.108}$$

$$\rho \geq p_t, \tag{2.109}$$

$$\rho \geq p_r + 2p_t. \tag{2.110}$$

It is worth noticing that DEC condition implies WEC, and WEC implies NEC. Consequently, an interior solution is energy acceptable if it satisfies the DEC condition. It is even desirable that SEC be fulfilled.

2.7 Gravitational decoupling approach (GD)

Since the EFE are a coupled system of nonlinear differential equations, the task of finding exact solutions for them is not an easy task. Indeed, only for some specific situations analytical solutions with a certain physical relevance have been found [9]. One of them is the spherically symmetric space-time with perfect fluid $T_{\mu\nu}$ as a gravitational source. Then, if the perfect fluid (which we will call from here as "seed source") is coupled to complex forms of matter-energy to describe more realistic scenarios, in particular,

$$\tilde{T}_{\mu\nu} = T^{(s)}_{\mu\nu} + \alpha\theta_{\mu\nu}, \tag{2.111}$$

where α is a coupling constant and $\theta_{\mu\nu}$ is other gravitational source, whose effect on the source $T_{\mu\nu}^{(s)}$ [3] is controlled by α. The situation of solve the respective EFE for the source (2.111) can be though as it is almost impossible to obtain analytical solutions that can be interpreted easily. In this respect, the so-called Minimal Geometric Deformation (MGD), originally proposed [60,61] in the context of the Randall-Sundrum brane-world [62, 63] and extended to investigate new black hole solutions [64,65], has been used to produce brane world configurations from general relativistic perfect fluid solutions. Even exact and physically acceptable solutions for interior stellar distributions were successfully generated [66].

The idea of this approach is solve the EFE for Eq. (2.111) by solving the two following independent problems

$$G_{\mu\nu}^{(s)} = 8\pi T_{\mu\nu}^{(s)} \tag{2.112}$$

$$G_{\mu\nu}^* = 8\pi \theta_{\mu\nu}, \tag{2.113}$$

where $\{g_{\mu\nu}^{(s)}, T_{\mu\nu}^{(s)}\}$ and $\{g_{\mu\nu}^*, \theta_{\mu\nu}\}$ are obtained. In this sense, the effect of the source $\theta_{\mu\nu}$ over the "seed" source should be reflected in the geometric deformation measured by

$$g_{\mu\nu} \longrightarrow g_{\mu\nu}^{(s)} + \alpha g_{\mu\nu}^*. \tag{2.114}$$

where α is a constant that "controls" the influence the $\theta_{\mu\nu}$ over $T_{\mu\nu}^{(s)}$.

Explicitly, if one considers a static and spherically symmetric space-time sourced by Eq.

---

[3] **We will use the upperscript "s" to indicate that it refers to the seed source.**

(2.111) where

$$T_\nu^{\mu(s)} = diag(\rho^{(s)}, -p_r^{(s)}, -p_t^{(s)}, -p_t^{(s)}) \tag{2.115}$$

and

$$\theta_\nu^\mu = diag\left(\theta_0^0, \theta_1^1, \theta_2^2, \theta_3^3\right), \tag{2.116}$$

Eq. (2.1) leads to

$$8\pi\tilde{\rho} = -\frac{1}{r^2} + e^{-\lambda}\left(\frac{1}{r^2} - \frac{\lambda'}{r}\right) \tag{2.117}$$

$$8\pi\tilde{P}_r = -\frac{1}{r^2} + e^{-\lambda}\left(\frac{1}{r^2} + \frac{\nu'}{r}\right) \tag{2.118}$$

$$8\pi\tilde{P}_t = -\frac{e^{-\lambda}}{4}\left(-2\nu'' - \nu'^2 + \lambda'\nu' - 2\frac{\nu' - \lambda'}{r}\right), \tag{2.119}$$

where we have defined

$$\tilde{\rho} = \rho^{(s)} + \alpha\theta_0^0, \tag{2.120}$$

$$\tilde{P}_r = P_r^{(s)} + \alpha\theta_1^1, \tag{2.121}$$

$$\tilde{P}_t = P_t^{(s)} + \alpha\theta_2^2, \tag{2.122}$$

being $\tilde{\rho}$, $\tilde{P}_r$ and $\tilde{P}_t$ the effective density, radial and transverse pressure of system.

Note that, as

$$\nabla_\mu\tilde{T}^{\mu\nu} = 0, \tag{2.123}$$

and $\nabla_\mu T^{\mu\nu(s)} = 0$, the condition

$$\nabla_\mu \theta^{\mu\nu} = 0, \tag{2.124}$$

is automatically fulfilled, which indicates that there is no exchange of energy-momentum between the "seed solution" and the extra source $\theta_{\mu\nu}$ so the interaction is entirely gravitational.

2.7.1 Minimal Geometric Deformation (MGD)

In the framework of Minimal Decoupling, the effect of the source $\theta_{\mu\nu}$ is considered as a modification of the nature of the original fluid, so it is possible to encode this by modifying the line element given by Eq. (2.8) as follows

$$\nu \longrightarrow \xi + \alpha g, \tag{2.125}$$

$$e^\lambda \longrightarrow e^{-\mu} + \alpha f, \tag{2.126}$$

where $\{f, g\}$ are the so-called decoupling functions. We say that the deformation is minimal when $g = 0$ and $f \neq 0$, thus such effect is the *geometric deformation* on the radial metric. Then, this geometric deformation is inserted in the system Eqs.(2.120)-(2.122), obtaining two subsets of equations: one describing a seed sector sourced by the conserved energy-momentum tensor $T_{\mu\nu}^{(s)}$

$$8\pi\rho^{(s)} = \frac{1}{r^2} + e^{-\mu}\left(\frac{\mu'}{r} - \frac{1}{r^2}\right), \tag{2.127}$$

$$8\pi P_r^{(s)} = -\frac{1}{r^2} + e^{-\mu}\left(\frac{\nu'}{r} + \frac{1}{r^2}\right), \tag{2.128}$$

$$8\pi P_t^{(s)} = \frac{1}{4}e^{-\mu}\left(2\nu'' + \nu'^2 - \mu'\nu' + 2\frac{\nu' - \mu'}{r}\right), \tag{2.129}$$

and the other set corresponding to quasi-Einstein field equations sourced by $\theta_{\mu\nu}$

$$8\pi\theta_0^0 = -\frac{f}{r^2} - \frac{f'}{r}, \tag{2.130}$$

$$8\pi\theta_1^1 = -f\left(\frac{\nu'}{r} + \frac{1}{r^2}\right), \tag{2.131}$$

$$8\pi\theta_2^2 = -\frac{f}{4}\left(2\nu'' + \nu'^2 + 2\frac{\nu'}{r}\right) - \frac{f'}{4}\left(\nu' + \frac{2}{r}\right). \tag{2.132}$$

As we have seen before, the components of $\theta_{\mu\nu}$ satisfy the conservation equation $\nabla_\mu\theta_\nu^\mu = 0$, explicitly

$$(\theta_1^1)' - \frac{\nu'}{2}(\theta_0^0 - \theta_1^1) - \frac{2}{r}(\theta_2^2 - \theta_1^1) = 0. \tag{2.133}$$

We have to emphasize the importance of GD as a useful tool to find solutions of EFE. As it is well known, in static and spherically symmetric space-times sourced by anisotropic fluids, EFE reduce to three equations given by (2.120)-(2.122) and five unknowns, namely $\{\nu, \lambda, \tilde{\rho}, \tilde{P}_r, \tilde{P}_t\}$, which need two auxiliary conditions to be solved. Thus, as in the context of GD a seed solution is given, the number of degrees of freedom reduces to four and, as a consequence, only one extra condition is needed. Specifically, this condition has been implemented in the decoupling sector given by Eqs. (2.130)-(2.132) as some equation of state, which leads to a differential equation for the decoupling function f. In this work, we take an alternative route to obtain the decoupling function f called the complexity factor that we shall introduce in the next section as a supplementary condition.

2.8 Complexity of compact sources

The complexity for self-gravitating fluid distributions has been introduced recently based on the idea that the least complex gravitational system is the one supported by a homogeneous energy density distribution and isotropic pressure. Such definition arises from a scalar associated with the orthogonal splitting of Riemann Tensor developed by Bel [35]. In static and spherically symmetric space–times this scalar encodes the intuitive idea of complexity, specifically it is

$$Y_{TF} = 8\pi\Pi - \frac{4\pi}{r^3} \int_0^r \tilde{r}^3 \rho' d\tilde{r}. \tag{2.134}$$

Besides, the Tolman mass can be defined in terms of this scalar as follows [36, 67]

$$m_T = (m_T)_\Sigma \left(\frac{r}{r_\Sigma}\right)^3 + r^3 \int_r^{r_\Sigma} \frac{e^{(\nu+\lambda)/2}}{\tilde{r}} Y_{TF} d\tilde{r}. \tag{2.135}$$

It is worth mentioning that the "active" gravitational mass m_T depends directly on the complexity factor. This implies that it can suffer modifications produced by the energy density inhomogeneity and the anisotropy of the pressure. The features mentioned above give a solid argument to define the scalar complexity factor by means of this scalar.

Note that for a system with homogeneous energy density distribution and isotropic pressure the complexity factor Y_{TF} vanishes. It is not the only system for which this factor becomes zero. It is also zero when

$$\Pi = \frac{1}{2r^3} \int_0^r \tilde{r}^3 \rho' d\tilde{r}, \tag{2.136}$$

which provides a non–local equation of state that can be used as a complementary condition to

close the system of EFE (in fact, this condition has been implement with the MGD in a recent work in [68]). However, in this work we use a specific value for Y_{TF} as a complementary condition over the matter sector so we replace Eqs. (2.125), (2.126) in (2.134) and use the Eqs. (2.120)-(2.122) to obtain

$$
\begin{aligned}
\frac{\alpha \xi'}{4} f' \quad + \quad & \frac{\alpha}{2} \left(\xi'' - \frac{\xi'}{r} + \frac{\xi'^2}{2} \right) f \\
& + \frac{e^{-\mu}}{2} \left(\xi'' - \frac{\xi'}{r} + \frac{\xi'^2}{2} - \frac{\mu' \xi'}{2} \right) + Y_{TF} = 0.
\end{aligned}
\tag{2.137}
$$

The above equation allows to find the geometric deformation f due to the seed solution supplying the metric functions $\{\xi, \mu\}$ and Y_{TF} being able to be specified.

2.9 Gravitational Cracking

The concept of cracking for self-gravitating compact objects is related to the behavior of a stellar fluid distribution just after departure from equilibrium. Specifically, cracking occurs whenever the total non-vanishing radial force, appearing after the perturbation of the system, is directed inward in the inner part of the sphere and changes its direction at some radial value r less than the radius of the compact object. Likewise, the force can be directed outward in the inner part of fluid and it change of sign in the outer part; such a situation is known as *overturning*. It is necessary to clarify that cracking only refers to the trend of the compact object to split[4] since it is related to the problem of structure formation of the compact stellar object only at time scales smaller or almost equal to hydrostatic timescales [73–75]. We have to emphasizing that phenomena such as the collapse of the inner part or the expansion of the outer part can appear

---

[4]Examples of such " splittings" have been reported elsewhere [70–72].

from cracking and must be modeled through the integration of the entire set of Einstein's equations for finite times greater than hydrostatic time. Thus, cracking has a drastic influence in the evolution of the structure of a stellar compact object. For example, this situation can affect the star's spin evolution as a result of the redistribution of the interior mass, therefore causing changes in the moment of inertia, starquakes or generating high-energy emissions [76–79].

Regarding the causes that can generate cracking, Di Prisco et.al. [42,43] suggested that fluctuations of local anisotropy may be the crucial factor in the occurrence of cracking, which is in agreement with the fact that small fluctuations from local isotropy may lead to drastic changes in the evolution of the system for the dynamics of a locally anisotropic fluid [80]. Since we are interested in the possible scenarios of stellar evolution, where fluctuations of local isotropy are factible in a regimen of high density, we will focus on the intense magnetic field observed in compact objects like white dwarfs, neutron stars, or magnetic strange quark stars [81–84] (since the magnetic field acting over a Fermi gas produces local pressure anisotropy as a natural consequence of the spatial reorientation of spins [85–89]) and the viscosity [90–97], which can be present in high density matter.

One way to explore how the system departs from equilibrium is through a perturbation in the TOV given by (2.87). Then, in order to include such perturbation, we can define the total force per unit volume for each fluid element as

$$\mathcal{R} \equiv \frac{dp_r}{dr} + \frac{(\rho + p)(m + 4\pi r^3 p_r)}{r(r - 2m)} + \frac{2}{r}\Pi. \tag{2.138}$$

Note that when the system is in equilibrium $\mathcal{R} = 0$. So, in order to find situations where

cracking or overturning happens, we shall consider in this work only disturbances in which the entire material sector of the interior solution is disturbed, except for the radial pressure p_r, which does not change. These disturbances are such that $\tilde{\mathcal{R}} \neq 0^5$. In this sense, we formally consider $\{\alpha, \beta\}$ parameters in the interior solution, which can modify the TOV when they are disturbed. Specifically, $\tilde{\mathcal{R}}(\alpha + \delta\alpha, \beta + \delta\beta)$ up to first order, so

$$\tilde{\mathcal{R}} = \frac{\partial \tilde{\mathcal{R}}}{\partial \alpha}\delta\alpha + \frac{\partial \tilde{\mathcal{R}}}{\partial \beta}\delta\beta + \mathcal{O}(\delta\alpha^2, \delta\beta^2). \tag{2.139}$$

From the above equation it is clear that if cracking occurs, $\tilde{\mathcal{R}}$ changes sign in some value of r; that is, when $\tilde{\mathcal{R}}$ has at least a real root. Now, if $\delta\beta = -\Gamma\delta\alpha$, the cracking condition translates to the existence of Γ such that

$$\Gamma = \frac{\partial \tilde{\mathcal{R}}/\partial \tilde{\alpha}|_{\beta,\alpha}}{\partial \tilde{\mathcal{R}}/\partial \tilde{\beta}|_{\beta,\alpha}}. \tag{2.140}$$

Up to now we have reviewed the necessary theory that will allow us to find a new set of anisotropic solutions within the framework of GD and also analyze their stability. The details of such development is detailed in the next chapter.

---

[5]**The tilde notes that the total radial force is being perturbed.**

Chapter 3

Stellar models with like–Tolman IV complexity factor

In this chapter we detail the process used to construct a new family of stellar models based on the complexity factor as a supplementary condition to close the system of equations arising from the MGD. As a first step, we find the complexity factor of the Tolman IV solution, so replacing Eqs. (2.60)-(2.63) in (2.134) we obtain

$$Y_{TF} = \frac{r^2(A^2 + 2C^2)}{C^2(A^2 + 2r^2)^2},$$
(3.1)

which can be generalized to

$$Y_{TF} = \frac{a_1 r^2}{(a_2 + a_3 r^2)^2},$$
(3.2)

where a_1, a_2 and a_3 are dimensionless constants and a_2 must be a constant with dimension of a length squared. The complexity factor, Eq. (3.2), will be used as the condition to close the

system in the framework of GD and generate anisotropic models from isotropic seeds.

3.1 Model 1: like–Tolman IV solution

In this section we use the seed solution given by Eqs. (2.60) and (2.61) in (2.137) to obtain the geometric deformation f

$$f(r) = (A^2 + r^2)\left[c_1 + \frac{1}{\alpha}\left(\frac{a_1}{a_3\zeta(r)} - \frac{A^2 + 2C^2}{2C^2(A^2 + 2r^2)}\right)\right], \tag{3.3}$$

where c_1 is an integration constant with dimensions of the inverse of a length squared and $\zeta(r)$ is an auxiliary function with dimensions of a length squared (see Appendix, section B). Now, in order to ensure regularity in the matter sector, the constant c_1 must satisfy

$$c_1 = \frac{a_2 a_3 A^2 + 2a_2 a_3 C^2 - 2a_1 A^2 C^2}{2\alpha a_2 a_3 A^2 C^2}. \tag{3.4}$$

Replacing (3.3) in (2.126) and using (3.4) we arrive at

$$e^{-\lambda(r)} = \frac{(A^2 + r^2)(a_2\zeta(r) - a_1 A^2 r^2)}{a_2 A^2 \zeta(r)}. \tag{3.5}$$

Now, we can use the radial component metric (3.5) in the system (2.117)-(2.119) to obtain the matter sector

$$\tilde{\rho}(r) = \frac{1}{8\pi a_2 A^2 \zeta(r)^2}\left[a_1 A^4\left(3a_2 + a_3 r^2\right) + a_1 A^2 r^2\left(5a_2 + 3a_3 r^2\right) - 3a_2\zeta(r)^2\right], \tag{3.6}$$

$$\tilde{P}_r(r) = \frac{3a_2\zeta(r) - a_1 A^2(A^2 + 3r^2)}{8\pi a_2 A^2 \zeta(r)}, \tag{3.7}$$

$$\tilde{P}_t(r) = \frac{3a_2\zeta(r)^2 - a_1 a_2 A^4 - a_1 A^2 r^2\left(5a_2 + 3a_3 r^2\right)}{8\pi a_2 A^2 \zeta(r)^2}. \tag{3.8}$$

Thus, we found a new interior solution in the anisotropic regime given by (2.60), (3.5)-(3.8). Now, it is necessary to apply the matching conditions (2.78), (2.79) and (2.82) to this solution to obtain the following

$$a_1 = \frac{3a_2\zeta(R)}{A^2(A^2 + 3R^2)} \tag{3.9}$$

$$\frac{A^2}{R^2} = \frac{R - 3M}{M} = \frac{1}{u} - 3 \tag{3.10}$$

$$B^2 = 1 - \frac{3M}{R} = 1 - 3u. \tag{3.11}$$

It is important to note that from (3.10) and (3.11) it is clear that compactness satisfies $u = M/R < 1/3$, which corresponds to a more demanding condition when compared to the the Buchdahl's limit ($u < 4/9$) for isotropic solutions [69]. In consequence, the solutions allowed with this model should be less compact given that the interval $1/3 \leq u < 4/9$ is forbidden.

3.2 Model 2: like–Wyman IIa solution

For this case we consider the Wyman IIa (with $n = 2$) model given by (2.64) and (2.65) as seed solution and, following the same procedure that in the previous section, we obtain

$$f(r) = \frac{r^2}{2\alpha a_3}\left[\frac{a_1(a_3 A + a_2 B)}{a_2 B\zeta(r)} - \frac{2a_3 C}{(A - 3Br^2)^{2/3}}\right] - \frac{a_1}{2\alpha a_3^2}\chi(r), \tag{3.12}$$

from where

$$e^{-\lambda(r)} = \frac{1}{2a_3^2}\left[\frac{a_3 r^2\left(a_1 a_3 A + a_2 B\left(a_1 + 2a_3^2\right)\right)}{a_2 B\zeta(r)} + \frac{2a_2 a_3^2}{\zeta(r)} - a_1\chi(r)\right]. \tag{3.13}$$

Now, using (3.13) in the system (2.117)-(2.119) the matter sector reads

$$\tilde{\rho}(r) = \frac{a_1}{16\pi a_3^2}\left[\frac{\chi(r)}{r^2} - \frac{a_3\varrho_1(r)}{a_2 B\zeta(r)^2}\right]$$

(3.14)

$$\tilde{P}_r(r) = \frac{a_3 r^2 \mathcal{P}_1(r) - a_1 a_2 B\left(5Br^2 - A\right)\zeta(r)\chi(r)}{16\pi a_2 a_3^2 Br^2\left(Br^2 - A\right)\zeta(r)}$$

(3.15)

$$\tilde{P}_t(r) = \frac{a_3\mathcal{P}_2(r) - 4a_1 a_2 B^2\zeta(r)^2\chi(r)}{16\pi a_2 a_3^2 B\left(Br^2 - A\right)\zeta(r)^2},$$

(3.16)

where we have used the auxiliary functions $\{\zeta, \chi, \varrho_1, \mathcal{P}_1, \mathcal{P}_2\}$, which are defined in Appendix, section B. Now, using the continuity of the first and the second fundamental form leads to

$$a_1 = \frac{8a_2 a_3^2 B^2 R^2\zeta(R)}{(A - 5BR^2)\left[a_3 R^2(a_3 A + a_2 B) - a_2 B\zeta(R)\chi(R)\right]}$$

(3.17)

$$A^2 = \frac{B^2(5M - 2R)^2 R^4}{M^2}$$

(3.18)

$$B^2 = \frac{M^2}{4R^5(R - 2M)}.$$

(3.19)

Note that from Eq. (3.19) results $R > 2M$, which is in accordance with the restriction that any stable configuration should be greater than its Schwarzschild radius.

3.3   Model 3: like–Durgapal IV solution

In this case we consider the Durgapal IV model given by Eqs. (2.68)-(2.69) as a seed solution. It is worth mentioning that, in what follows, we shall use the auxiliary functions $\{\zeta, \eta_1, \beta_1, \beta_4, \beta_5, \beta_8, \beta_{11}, \varrho_2, \mathcal{P}_3, \mathcal{P}_4\}$ defined in the Appendix, section B.

Following the same procedure of the previous two models, we obtain

$$
\begin{aligned}
f(r) &= \frac{r^2}{56\alpha a_3^3 C \beta_1(r)^2} \left[7a_1 \left(-a_3 C^3 r^2 + \frac{2(a_2 C - a_3)^3}{a_2 \zeta(r)} + 2C^2(2a_2 C - 3a_3) \right) \right. \\
&\qquad\qquad \left. + 8a_3^3 C^2 \left(Cr^2 + 10 - \frac{7B}{(5Cr^2 + 1)^{2/5}} \right) \right] \\
&\qquad - \frac{3a_1(a_3 - a_2 C)^2 \chi(r)}{4\alpha a_3^4 \beta_1(r)^2},
\end{aligned}
\tag{3.20}
$$

and the radial component metric reads

$$
e^{-\lambda(r)} = \frac{a_3 \eta_1(r) - 6a_1 a_2 C(a_3 - a_2 C)^2 \zeta(r) \chi(r)}{8a_2 a_3^4 C \beta_1(r)^2 \zeta(r)}.
\tag{3.21}
$$

Now, from Eqs. (2.117)-(2.119) we obtain

$$
\begin{aligned}
\tilde{\rho}(r) &= \frac{1}{64\pi a_2 a_3^4 C r^2 \beta_1(r)^3 \zeta(r)^2} \left[a_3 r^2 \varrho_2(r) + \right. \\
&\qquad\qquad \left. - 6a_1 a_2 C \beta_4(r)(a_3 - a_2 C)^2 \zeta(r)^2 \chi(r) \right],
\end{aligned}
\tag{3.22}
$$

$$
\tilde{P}_r(r) = \frac{\mathcal{P}_3(r)}{64\pi a_2 a_3^4 C r^2 \beta_1(r)^3 \zeta(r)},
\tag{3.23}
$$

$$
\tilde{P}_t(r) = \frac{\mathcal{P}_4(r)}{32\pi a_2 a_3^4 C \beta_1(r)^3 \zeta(r)^2}.
\tag{3.24}
$$

Applying the continuity of the first and the second fundamental form leads to

$$
a_1 = \frac{8a_2 a_3^4 C^2 R^2 \left(6 - C R^2 \beta_5(R) \right) \zeta(R)}{\beta_8(R) \left[a_3 R^2 \beta_{11}(R) + 6a_2 C(a_3 - a_2 C)^2 \zeta(R) \chi(R) \right]}
\tag{3.25}
$$

$$
A = \frac{1 - \frac{2M}{R}}{\left(\frac{M}{4R - 9M} + 1 \right)^4}
\tag{3.26}
$$

$$
C = \frac{M}{R^2(4R - 9M)}.
\tag{3.27}
$$

For this case, it is clear that from Eqs. (3.26) and (3.27), the solution must satisfy $M/R < 4/9$ (which coincides with the Buchdahl's limit for isotropic solutions).

3.4   Model 4: like–Heintzmann IIa solution

In this section we consider the metric components of the Heintzmann IIa solution given by Eqs. (2.72) and (2.73) as seed solution. Implementing the same procedure as before we obtain

$$f(r) = \frac{r^2}{6\alpha B\gamma_1(r)}\left[\frac{9B^2C}{\sqrt{4Br^2+1}} + 3B^2 - \frac{2a_1\left(2a_2^2B^2 + a_2a_3B\gamma_2(r) + a_3^2\right)}{a_2a_3^2\zeta(r)}\right] \\ -\frac{2a_1(a_3 - a_2B)\chi(r)}{3a_3^3\alpha\gamma_1(r)}, \tag{3.28}$$

where γ_1 and γ_2 are auxiliary functions defined in the Appendix, section B. It is compulsory to mention that in this section we shall use the list of auxiliary functions $\{\zeta, \eta_2, \gamma_1, \gamma_3, \gamma_6, \gamma_7, \gamma_9, \varrho_3, \mathcal{P}_5, \mathcal{P}_6\}$ defined in the Appendix, section B.

Now, by using Eq. (3.28) we obtain the radial metric component as follows

$$e^{-\lambda(r)} = \frac{a_3\eta_2(r) + 2a_1a_2B(a_2B - a_3)\zeta(r)\chi(r)}{3a_2a_3^3B\gamma_1(r)\zeta(r)}. \tag{3.29}$$

Then, using the system of Eqs. (2.117)-(2.119), it leads to

$$\tilde{\rho} = \frac{2a_1a_2B\gamma_3(r)(a_2B - a_3)\zeta(r)^2\chi(r) + a_3r^2\varrho_3(r)}{24\pi a_2a_3^3Br^2\gamma_1(r)^2\zeta(r)^2}, \tag{3.30}$$

$$\tilde{P}_r = \frac{\mathcal{P}_5(r)}{24\pi a_2a_3^3Br^2\gamma_1(r)^2\zeta(r)}, \tag{3.31}$$

$$\tilde{P}_t = \frac{\mathcal{P}_6(r)}{24\pi a_2a_3^3B\gamma_1(r)^2\zeta(r)^2}. \tag{3.32}$$

From the matching conditions we have

$$a_1 = -\frac{3a_2 a_3^3 B^2 R^2 \gamma_7(R)\zeta(R)}{\gamma_6(R)\left[a_3 R^2 \gamma_9(R) - 2a_2 B(a_2 B - a_3)\zeta(R)\chi(R)\right]} \tag{3.33}$$

$$A^2 = -\frac{(7M - 3R)^3}{27R(R - 2M)^2} \tag{3.34}$$

$$B^2 = \frac{M^2}{R^4(3R - 7M)^2}. \tag{3.35}$$

Note that from (3.34) and (3.35) results $R > 2M$, which, as mentioned before, is in accordance with stable configuration of an stellar compact object. We also have that $u < 3/7 < 4/9$, which corresponds to less compact solutions than the allowed by the Buchdahl's limit [69].

Once new solutions have been found in this work the next step is study their stability. In order to reach that, in the next section the total perturbed radial force for each model is found.

3.5 Total perturbed radial force of stellar models with like –Tolman IV complexity factor

In this section we find the total perturbed radial force for each model found in the previous chapter. Such force is a necessary requirement to analyze the stability of self gravitating spheres.

3.5.1 Model 1: like–Tolman IV solution

Let us rewrite the anisotropic *Model 1* found in Section 3.1 as follows

$$e^\nu = B^2 \left(\frac{r^2}{A^2} + 1 \right), \tag{3.36}$$

$$e^{-\lambda} = \frac{(A^2 + r^2)\left(a_2 \zeta(r) - a_1 A^2 r^2\right)}{a_2 A^2 \zeta(r)}, \tag{3.37}$$

$$\rho = \frac{a_1 A^2 \varrho(r) - 3a_2 \zeta(r)^2}{8\pi a_2 A^2 \zeta(r)^2}, \tag{3.38}$$

$$p_r = \frac{3a_2 \zeta(r) - a_1 A^2 (A^2 + 3r^2)}{8\pi a_2 A^2 \zeta(r)}, \tag{3.39}$$

$$\Pi = \frac{a_1 r^2 \left(2a_2 - a_3 A^2\right)}{8\pi a_2 \zeta(r)^2}, \tag{3.40}$$

$$m = \frac{r^3 \left(a_1 A^4 + a_1 A^2 r^2 - a_2 \zeta(r)\right)}{2A^2 a_2 \zeta(r)}, \tag{3.41}$$

where m was calculated with Eq. (2.21), $\zeta(r)$ and $\varrho(r)$ are auxiliary functions (see Appendix C).

Now, it is necessary to use (3.9) in order to express the solution in the following way

$$\rho = \frac{\mathcal{P}_1(r)}{8\pi A^2 \left(A^2 + 3R^2\right) \zeta(r)^2} \tag{3.42}$$

$$p_r = \frac{3(r - R)(r + R)\left(a_3 A^2 - 3a_2\right)}{8\pi A^2 \left(A^2 + 3R^2\right) \zeta(r)} \tag{3.43}$$

$$\Pi = -\frac{3r^2 \left(a_3 A^2 - 2a_2\right)\left(a_2 + a_3 R^2\right)}{8\pi A^2 \left(A^2 + 3R^2\right) \zeta(r)^2} \tag{3.44}$$

$$m = \frac{3r^3 \mathcal{P}_2(r)}{A^2 \left(A^2 + 3R^2\right) \zeta(r)}, \tag{3.45}$$

where $\mathcal{P}_1(r)$ and $\mathcal{P}_2(r)$ are auxiliary functions defined in Appendix B.

Note that from the observation of the whole model the constants a_1 and a_3 are dimensionless,

whereas A has units of a length and a_2 has units of a length squared. Then, it is convenient, for our analysis, to define the dimensionless quantities

$$\alpha = \frac{A}{R} \tag{3.46}$$

$$x = \frac{r}{R} \tag{3.47}$$

$$\beta = \frac{a_2}{R^2}, \tag{3.48}$$

in terms of which the matter sector $\{\rho, p_r, \Pi, m\}$ can be rewritten depending on the auxiliary functions $\mathcal{P}_1(\alpha, \beta, x)$, $\mathcal{P}_2(\alpha, \beta, x)$ and $\varsigma(\beta, x)$ (see Appendix C) as

$$\rho = \frac{\mathcal{P}_1(\alpha, \beta, x)}{8\pi R^4 \alpha^2 (\alpha^2 + 3)\varsigma(\beta, x)^2}$$

$$= \frac{3}{8\pi R^2} \hat{\rho}(\alpha, \beta, x) \tag{3.49}$$

$$p_r = \frac{3}{8\pi R^2} \left(\frac{(x^2 - 1)(a_3\alpha^2 - 3\beta)}{\alpha^2 (\alpha^2 + 3)(\beta + a_3 x^2)} \right)$$

$$= \frac{3}{8\pi R^2} \hat{p}_r(\alpha, \beta, x) \tag{3.50}$$

$$\Pi = \frac{3}{8\pi R^2} \left(\frac{x^2 (\beta + a_3)(2\beta - a_3\alpha^2)}{\alpha^2 (\alpha^2 + 3)(\beta + a_3 x^2)^2} \right)$$

$$= \frac{3}{8\pi R^2} \hat{\Pi}(\alpha, \beta, x) \tag{3.51}$$

$$m = R \left(\frac{x^3 \mathcal{P}_2(\alpha, \beta, x)}{2R^2 \alpha^2 (\alpha^2 + 3)\varsigma(\beta, x)} \right)$$

$$= R\hat{m}. \tag{3.52}$$

Now, assuming a_3 as a fixed parameter, we can proceed to perturb the matter sector through the

variation of the parameters $\{\alpha, \beta\}$

$$\alpha \to \tilde{\alpha} = \alpha + \delta\alpha \tag{3.53}$$

$$\beta \to \tilde{\beta} = \alpha + \delta\beta, \tag{3.54}$$

where the tilde indicates that the quantity is being perturbed. In this work we perturb the entire matter sector except for the radial pressure p_r, so that the TOV is different from zero. Namely, the system departs from hydrostatic equilibrium. In other words, the relations (3.49)-(3.52) result in

$$\tilde{\mathcal{R}} = \frac{1}{2}\frac{d\hat{p}_r}{dx} + \frac{\left(\hat{\rho}(\tilde{\alpha}, \tilde{\beta}, x) + \hat{p}_r\right)\left(\hat{m}(\tilde{\alpha}, \tilde{\beta}, x) + \frac{3}{2}x^3\hat{p}_r\right)}{2x^2\left(1 - \frac{2\hat{m}(\tilde{\alpha}, \tilde{\beta}, x)}{x}\right)} + \frac{1}{x}\hat{\Pi}(\tilde{\alpha}, \tilde{\beta}, x), \tag{3.55}$$

where $\hat{p}_r = \hat{p}_r(\alpha, \beta, x)$ and

$$\tilde{\mathcal{R}} \equiv \frac{4\pi R^3}{3}\mathcal{R}. \tag{3.56}$$

Note that if cracking occurs, $\tilde{\mathcal{R}}$ must have a zero in the interval $x \in (0, 1)$.

3.5.2 Model 2: like–Wyman IIa solution

From section 3.2, the model reads

$$e^{\nu} = (A - Br^2)^2, \tag{3.57}$$

$$e^{-\lambda} = \frac{1}{2a_3^2}\left[\frac{a_3r^2\left(Aa_1a_3 + a_2B\left(a_1 + 2a_3^2\right)\right)}{a_2B\zeta(r)} + \frac{2a_2^2a_3B}{\zeta(r)} - a_1\chi(r)\right], \tag{3.58}$$

$$\rho = \frac{a_1}{16\pi a_3^2}\left[\frac{\chi(r)}{r^2} - \frac{a_3\tau(r)}{a_2B\zeta(r)^2}\right], \tag{3.59}$$

$$p_r = \frac{a_3r^2\mathcal{P}_3(r) - a_1a_2B\left(5Br^2 - A\right)\zeta(r)\chi(r)}{16\pi a_2a_3^2Br^2\left(Br^2 - A\right)\zeta(r)}, \tag{3.60}$$

$$\Pi = \frac{a_1}{16\pi a_3^2}\left(\frac{a_3\left(a_3r^2(a_3A + 4a_2B) + a_2^2B\right)}{a_2B\chi(r)^2} - \frac{\chi(r)}{r^2}\right), \tag{3.61}$$

$$m = \frac{a_1r}{4a_3^2}\left(\chi(r) - \frac{a_3r^2(a_3A + a_2B)}{a_2B\zeta(r)}\right), \tag{3.62}$$

where $\chi(r)$, $\tau(r)$ and $\mathcal{P}_3(r)$ are auxiliary functions (see Appendix C). Now we introduce the following quantities

$$x = \frac{r}{R} \tag{3.63}$$

$$\alpha = BR^2 \tag{3.64}$$

$$\beta = a_3R^2, \tag{3.65}$$

from where

$$\begin{aligned}
\rho &= \frac{\alpha}{2\pi R^2}\left(\frac{(a_2 + \beta)\vartheta_1(\alpha, \beta, x)}{x^2(A - 5\alpha)\zeta(\beta, x)^2\vartheta_2(\alpha, \beta, x)}\right) \\
&= \frac{\alpha}{2\pi R^2}\hat{\rho}
\end{aligned} \tag{3.66}$$

$$p_r = \frac{\alpha}{2\pi R^2} \frac{\vartheta_3(\alpha, \beta, x)^{-1}}{x^2 \zeta(\beta, x)\vartheta_2(\alpha, \beta, x)} \Bigg[$$
$$\beta x^2 \left(x^2 - 1\right)(A\beta + \alpha a_2)(A\beta + 5\alpha a_2)$$
$$+ \alpha a_2(a_2 + \beta)\zeta(\beta, x)\vartheta_4(\alpha, \beta, x)\Bigg]$$
$$= \frac{\alpha}{2\pi R^2}\hat{p}_r \tag{3.67}$$
$$\Pi = \frac{\alpha}{2\pi R^2}\left(\frac{(a_2 + \beta)\vartheta_5(\alpha, \beta, x)}{x^2(A - 5\alpha)\zeta(\beta, x)^2 \vartheta_6(\alpha, \beta, x)}\right)$$
$$= \frac{\alpha}{2\pi R^2}\hat{\Pi} \tag{3.68}$$
$$m = R\left(\frac{2\alpha x(a_2 + \beta)\vartheta_7(\alpha, \beta, x)}{(5\alpha - A)\zeta(\beta, x)\vartheta_6(\alpha, \beta, x)}\right)$$
$$= R\hat{m}, \tag{3.69}$$

where the auxiliary functions $\{\vartheta_1, \vartheta_2, \vartheta_3, \vartheta_4, \vartheta_5, \vartheta_6, \vartheta_7\}$ and $\zeta(\beta, x)$ are defined in Appendix C.

Considering A and a_2 we proceed to apply (3.53), (3.54) in (2.139) to obtain

$$\tilde{\mathcal{R}} = \frac{2\alpha}{3}\frac{d\hat{p}_r}{dx} + \frac{2}{3}\frac{\left(\tilde{\alpha}\hat{\rho}(\tilde{\alpha}, \tilde{\beta}, x) + \alpha\hat{p}_r\right)\left(\hat{m}(\tilde{\alpha}, \tilde{\beta}, x) + 2\alpha x^3 \hat{p}_r\right)}{x^2\left(1 - \frac{2\hat{m}(\tilde{\alpha}, \tilde{\beta}, x)}{x}\right)}$$
$$+ \frac{4\tilde{\alpha}}{3}\frac{1}{x}\hat{\Pi}(\tilde{\alpha}, \tilde{\beta}, x), \tag{3.70}$$

where $\hat{p}_r = \hat{p}_r(\alpha, \beta, x)$ and (3.56).

3.5.3 Model 3: like–Durgapal IV solution

From section 3.3 the relevant information reads

$$e^{\nu} = A \left(Cr^2 + 1 \right)^4, \tag{3.71}$$

$$e^{-\lambda} = \frac{1}{8a_2 a_3^4 C \left(Cr^2 + 1 \right)^2 \zeta(r)} \left[6a_1 a_2 C \ln(a_2)(a_3 - a_2 C)^2 \zeta(r) \right.$$
$$\left. - 6a_1 a_2 C (a_3 - a_2 C)^2 \zeta(r) \ln \zeta(r) + a_3 \eta_1(r) \right], \tag{3.72}$$

$$\rho = \frac{1}{64\pi a_2 a_3^4 C r^2 \left(Cr^2 + 1 \right)^3 \zeta(r)^2} \left[a_3 r^2 \eta_2(r) \right.$$
$$\left. - 6a_1 a_2 C \left(3Cr^2 - 1 \right) (a_3 - a_2 C)^2 \zeta(r)^2 \chi(r) \right], \tag{3.73}$$

$$p_r = \frac{\mathcal{P}_4(r)}{64\pi a_2 a_3^4 C r^2 \left(Cr^2 + 1 \right)^3 \zeta(r)}, \tag{3.74}$$

$$\Pi = \frac{1}{64\pi \left(Cr^2 + 1 \right)^3} \left[\frac{a_1 \mathcal{P}_5(r)}{a_2 a_3^3 C \zeta(r)^2} - 8C^2 r^2 (3 + Cr^2) \right.$$
$$\left. - \frac{6a_1 \left(3Cr^2 + 1 \right) (a_3 - a_2 C)^2 \chi(r)}{a_3^4 r^2} \right], \tag{3.75}$$

$$m = \frac{r}{16 \left(Cr^2 + 1 \right)^2} \left[\frac{2a_1 r^2}{a_2 \zeta(r) C} + r^2 \left(\frac{a_1 \eta_4(r)}{a_3^3 \zeta(r)} + 8C \left(Cr^2 + 2 \right) \right) \right.$$
$$\left. + \frac{6a_1 (a_3 - a_2 C)^2 \chi(r)}{a_3^4} \right], \tag{3.76}$$

where the functions $\eta_1(r), \eta_2(r), \eta_4(r), \mathcal{P}_4(r), \mathcal{P}_5(r)$ are defined in Appendix C.

Now from the metrics (3.71), (3.72) and the resulting matter sector we can infer that is convenient to carry out the following parameterization

$$x = \frac{r}{R} \tag{3.77}$$

$$\alpha = CR^2 \tag{3.78}$$

$$\beta = a_3 R^2, \tag{3.79}$$

while the parameters A and a_2 turn out to be dimensionless. Then the matter sector takes the form

$$
\begin{aligned}
\rho &= \frac{\alpha}{8\pi R^2 \left(\alpha x^2 + 1\right)^3} \left[\alpha x^2 \left(\alpha x^2 + 3\right) + 6 \right. \\
&\quad + \frac{(\alpha(\alpha + 3) - 6)\beta(a_2 + \beta)\varrho_1(\alpha, \beta, x)}{(9\alpha + 1)\zeta(\beta, x)^2 \varrho_2(\alpha, \beta, x)} \\
&\quad \left. - \frac{6\alpha a_2 \left(3\alpha x^2 - 1\right) \varrho_3(\alpha, \beta, x)\chi(\beta, x)}{(9\alpha + 1)x^2 \varrho_2(\alpha, \beta, x)} \right] \\
&= \frac{\alpha}{8\pi R^2}\hat{\rho} && (3.80) \\
p_r &= \frac{1}{8\pi R^2 x^2} \left(\frac{\left(1 + 9x^2\alpha\right) \varrho_4(\alpha, \beta)}{(9\alpha + 1)\left(\alpha x^2 + 1\right)^3 \zeta(\beta, x)\varrho_2(\alpha, \beta)} - 1 \right) \\
&= \frac{1}{8\pi R^2}\hat{p}_r && (3.81) \\
\Pi &= -\frac{\alpha}{8\pi R^2 \left(\alpha x^2 + 1\right)^3} \left[\alpha x^2 \left(\alpha x^2 + 3\right) \right. \\
&\quad + \frac{(6 - \alpha(\alpha + 3))\beta(a_2 + \beta)\varrho_{10}(\alpha, \beta, x)}{(9\alpha + 1)\zeta(\beta, x)^2 \varrho_2(\alpha, \beta, x)} \\
&\quad \left. + \frac{6\alpha a_2 \left(3\alpha x^2 + 1\right) \varrho_3(\alpha, \beta, x)\chi(\beta, x)}{x^2(9\alpha + 1)\varrho_2(\alpha, \beta, x)} \right] \\
&= \frac{\alpha}{8\pi R^2}\hat{\Pi} && (3.82) \\
m &= R \left(\frac{\alpha x \varrho_{11}(\alpha, \beta, x)}{2(9\alpha + 1)\left(\alpha x^2 + 1\right)^2 \zeta(\beta, x)\varrho_2(\alpha, \beta, x)} \right) \\
&= R\hat{m}, && (3.83)
\end{aligned}
$$

where the functions $\{\varrho_1, \varrho_2, \varrho_3, \varrho_4, \varrho_{10}, \varrho_{11}\}$ and the functions $\chi(\beta, x)$ are defined in Appendix C.

Now, we proceed to apply the perturbation on the parameters α and β through of (3.53),

(3.54) and (2.139) so that

$$
\tilde{\mathcal{R}} = \frac{1}{6}\frac{d\hat{p}_r}{dx} + \frac{\left(\tilde{\alpha}\hat{\rho}(\tilde{\alpha},\tilde{\beta},x) + \hat{p}_r\right)\left(\hat{m}(\tilde{\alpha},\tilde{\beta},x) + \frac{1}{2}\hat{p}_r x^3\right)}{6x^2\left(1 - \frac{2\hat{m}(\tilde{\alpha},\tilde{\beta},x)}{x}\right)}
$$
$$
+ \frac{2\tilde{\alpha}}{3x}\tilde{\Pi}(\tilde{\alpha},\tilde{\beta},x), \tag{3.84}
$$

where $\hat{p}_r = \hat{p}_r(\alpha,\beta,x)$ and (3.56).

3.5.4   Model 4: like–Heintzmann IIa

From section 3.4 we have

$$
e^\nu = A^2\left(Br^2 + 1\right)^3, \tag{3.85}
$$
$$
e^{-\lambda} = \frac{a_3\varphi_1(r) + 2a_1a_2B(a_2B - a_3)\zeta(r)\chi(r)}{3a_2a_3^3B\left(Br^2 + 1\right)\zeta(r)}, \tag{3.86}
$$
$$
\rho = \frac{1}{24\pi a_2a_3^3Br^2\left(Br^2 + 1\right)^2\zeta(r)^2}\Big[a_3r^2\varphi_2(r)
$$
$$
+ 2a_1a_2B\left(Br^2 - 1\right)(a_2B - a_3)\zeta(r)^2\chi(r)\Big], \tag{3.87}
$$
$$
p_r = \frac{2a_1a_2B\left(7Br^2 + 1\right)(a_2B - a_3)\zeta(r)\chi(r)}{24\pi a_2a_3^3Br^2\left(Br^2 + 1\right)^2\zeta(r)} - \frac{a_3r^2\varphi_3(r)}{24\pi a_2a_3^3Br^2\left(Br^2 + 1\right)^2\zeta(r)} \tag{3.88}
$$

$$
\Pi = \frac{1}{24\pi a_2a_3^3Br^2\left(Br^2 + 1\right)^2\zeta(r)^2}\Big[a_1a_3r^2\varphi_4(r)
$$
$$
- 2a_1a_2B\left(2Br^2 + 1\right)(a_3 - a_2B)\zeta(r)^2\chi(r) - 3a_2a_3^3B^3r^4\zeta(r)^2\Big], \tag{3.89}
$$
$$
m = \frac{a_3\varphi_5(r) + 2a_1a_2B(a_2B - a_3)\zeta(r)\chi(r)}{3a_2a_3^3B\left(Br^2 + 1\right)\zeta(r)}, \tag{3.90}
$$

where the auxiliary functions $\{\varphi_1, \varphi_2, \varphi_3, \varphi_4, \varphi_5\}$ are defined in Appendix C. In order to express the results in a more convenient manner, we introduce

$$x = \frac{r}{R} \tag{3.91}$$

$$\alpha = BR^2 \tag{3.92}$$

$$\beta = a_3 R^2, \tag{3.93}$$

from where

$$
\begin{aligned}
\rho &= \frac{\alpha}{8\pi R^2 \left(\alpha x^2 + 1\right)^2} \left[\alpha x^2 + 3 - \frac{(\alpha - 5)\beta(a_2 + \beta)\gamma_1(\alpha, \beta, x)}{(7\alpha + 1)\zeta(\beta, x)^2 \gamma_2(\alpha, \beta, x)}\right. \\
&\qquad \left. - \left(\alpha x^2 - 1\right) \Upsilon(\alpha, \beta, x)\right] \\
&= \frac{\alpha}{8\pi R^2} \hat{\rho} \tag{3.94} \\
p_r &= \frac{\alpha}{8\pi R^2 \left(\alpha x^2 + 1\right)^2} \left[5 - \alpha x^2 + \frac{\gamma_3(\alpha, \beta, x) \left(7\alpha x^2 + 1\right) \gamma_4(\alpha, \beta, x)}{(7\alpha + 1)\zeta(\beta, x)\gamma_2(\alpha, \beta, x)}\right. \\
&\qquad \left. - \left(7\alpha x^2 + 1\right) \Upsilon(\alpha, \beta, x)\right] \\
&= \frac{\alpha}{8\pi R^2} \hat{p}_r \tag{3.95}
\end{aligned}
$$

$$
\begin{aligned}
\Pi &= \frac{\alpha}{8\pi R^2 \left(\alpha x^2 + 1\right)^2} \left[-\alpha x^2 - \frac{\beta\gamma_3(\alpha, \beta, x)\gamma_5(\alpha, \beta)}{(7\alpha + 1)\zeta(\beta, x)^2 \gamma_2(\alpha, \beta)}\right. \\
&\qquad \left. - \left(2\alpha x^2 + 1\right) \Upsilon(\alpha, \beta, x)\right] \\
&= \frac{\alpha}{8\pi R^2} \hat{\Pi} \tag{3.96} \\
m &= \frac{\alpha x R}{2 \left(\alpha x^2 + 1\right)} \left[x^2 + \frac{\beta x^2 \gamma_3(\alpha, \beta, x)\gamma_4(\alpha, \beta, x)}{(7\alpha + 1)\zeta(\beta, x)\gamma_2(\alpha, \beta, x)} + x^2 \Upsilon(\alpha, \beta, x)\right] \\
&= R\hat{m}. \tag{3.97}
\end{aligned}
$$

Then if we perturb the parameters α and β in the way of (3.53) and (3.54) and use the equation (2.139), we have

$$\tilde{\mathcal{R}} = \frac{\alpha}{6}\frac{d\hat{p}_r}{dx} + \frac{\left(\tilde{\alpha}\hat{\rho}(\tilde{\alpha},\tilde{\beta},x) + \alpha\hat{p}_r\right)\left(\hat{m}(\tilde{\alpha},\tilde{\beta},x) + \frac{\alpha}{2}\hat{p}_r x^3\right)}{6x^2\left(1 - \frac{2\hat{m}(\tilde{\alpha},\tilde{\beta},x)}{x}\right)} + \frac{\tilde{\alpha}}{3x}\hat{\Pi}, \qquad (3.98)$$

where $\hat{p}_r = \hat{p}_r(\alpha,\beta,x)$ and with (3.56).

Chapter 4

Results and discussions

The present chapter is dedicated to verify the physical acceptability of the stellar models obtained in the chapter 3 and their stability in the context of gravitational cracking. For such purposes we shall use the compactness parameters given in Table 4.1 and a set of suitable values of a_2 and a_3 in order to discuss to what extent our solutions are adequate to describe the X-ray pulsars belonging to the binary star systems SMC X-1 and Cen X-3[1] [98].

Compact start	$M/M_{\odot}$	$R(km)$	$u = M/R$	$\rho(0)/\rho(R)$	$z(R)$
SMC X-1 [98]	1.04	8.301	0.19803	1.4659 [99]	0.286776
Cen X-3 [100]	1.49	10.8	0.2035	1.915 [101]	0.298592

Table 4.1: Physical parameters for the compact stars of the systems SMC X-1 and Cen X-3.

4.1 Metrics

In Figures 4.1 and 4.2 the metric functions for compactness parameters indicated in the legend are shown. Note that e^{ν} is a monotonously increasing function of r with $e^{\nu(0)} = constant$.

---

[1]These systems consist of a X ray source (pulsar) with a blue supergiant star as companion.

While $e^{-\lambda}$ is monotonously decreasing with $e^{-\lambda(0)} = 1$, as expected.

(a) (b) (c)

(d)
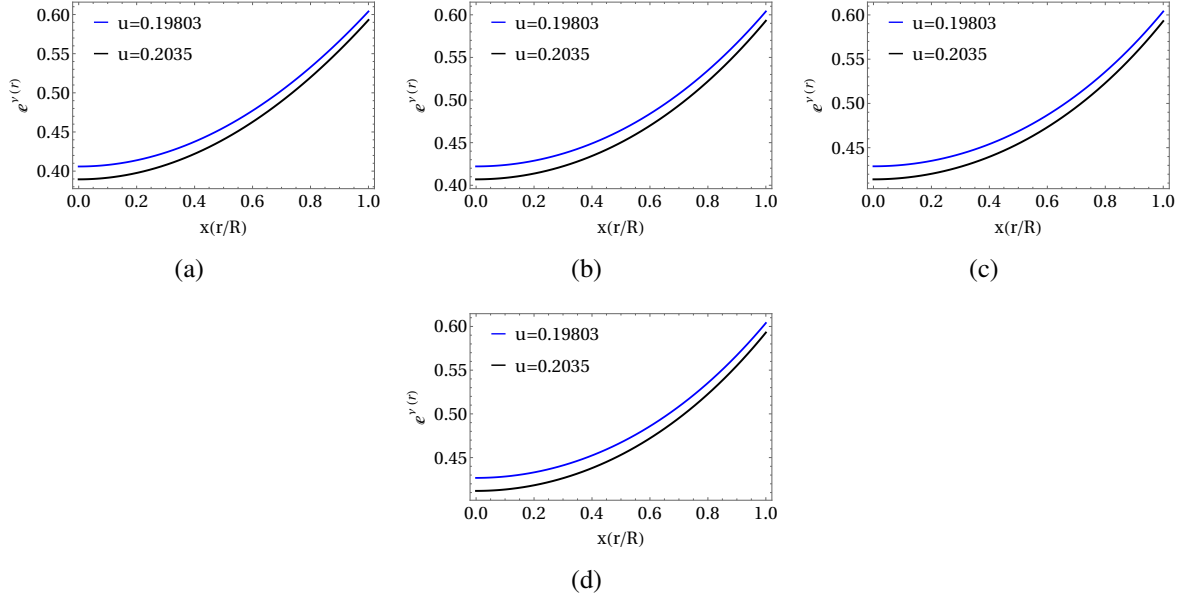
Figure 4.1: e^{ν} for Model 1 (a), Model 2 (b), Model 3 (c) and Model 4 (d).

4.2 Matter sector

In Figures 4.3, 4.4 and 4.5 we show the profile of the physical quantities $\tilde{\rho}$, $\tilde{P}_r$ and $\tilde{P}_t$ as a function of the radial coordinate r for the values of the parameters in the legend. It is important to note that all these quantities fulfill the physical requirements discussed before in section 2.6 for all the parameters involved, that is $\tilde{\rho}$, $\tilde{P}_r$ and $\tilde{P}_t$ are finite at the center and decrease monotonously toward the surface. Furthermore, $\tilde{P}_t(0) = \tilde{P}_r(0)$ and $\tilde{P}_t(r) > \tilde{P}_r(r)$ for all $r > 0$ as expected (see Figure 4.6).
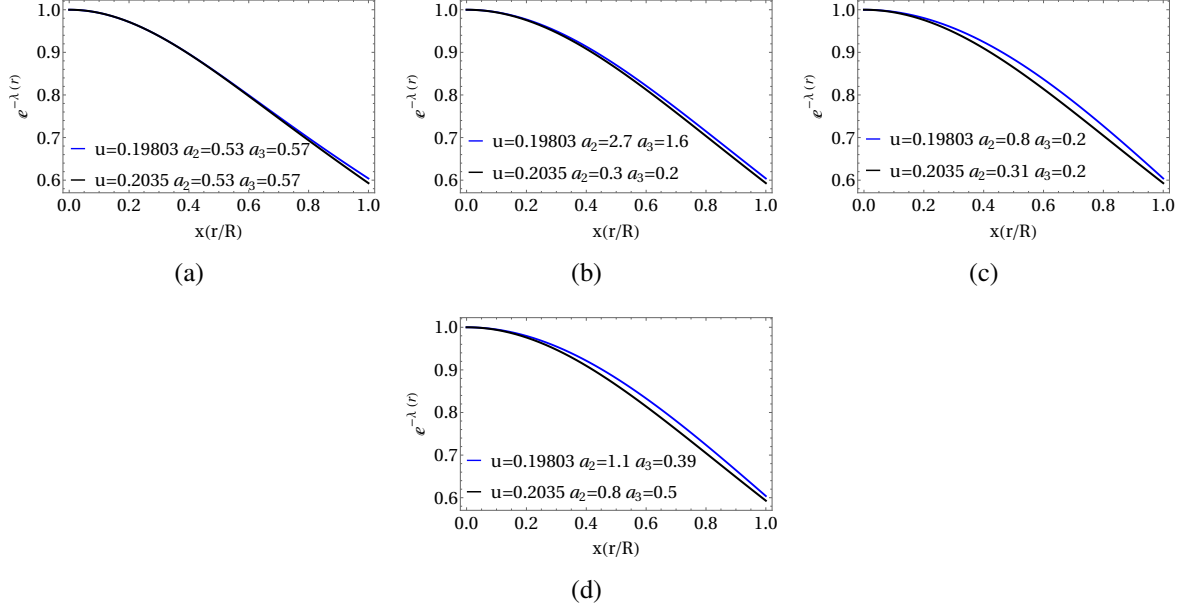
Figure 4.2: $e^{-\lambda}$ for Model 1 (a), Model 2 (b), Model 3 (c) and Model 4 (d).

4.3 Energy conditions and causality

The matter sector of a suitable stellar model must satisfy the dominant energy condition (DEC) in order to avoid violation of causality. The DEC for these models requires

$$\tilde{\rho} - \tilde{P}_r \geq 0 \tag{4.1}$$

$$\tilde{\rho} - \tilde{P}_t \geq 0. \tag{4.2}$$

From Figures 4.7 and 4.8 it can be seen that all the models satisfy DEC for all the parameters involved.

Besides, in Figures 4.9 and 4.10 we can observe that the radial and tangential fluid sound velocities are less than unity, as required (remember that we are assuming $c = 1$).

Figure 4.3: $\tilde{\rho}$ as a function of r for Model 1: (a) u = 0.19803, (b) u = 0.2035, Model 2: (c) u = 0.19803, (d) u = 0.2035, Model 3: (e) u = 0.19803, (f) u = 0.2035, Model 4: (g) u = 0.19803, (h) u = 0.2035.

4.4   Redshift and density ratio

In the previous section it has been demonstrated that the four models fulfill the basic physical requirements necessary to consider them as acceptable interior fluid solution for the compactness parameter of both SMC X-1 and Cen X-3 (see Table 4.1). We can now explore which models are more adequate to describe the compact objects under consideration. In this regard, we study the redshift $z = e^{-\nu/2} - 1$ and the density ratio $\tilde{\rho}(0)/\tilde{\rho}(R)$ to each model and com-

Figure 4.4: $\tilde{P}_r(r)$ as a function of r for Model 1: (a) u = 0.19803, (b) u = 0.2035, Model 2: (c) u = 0.19803, (d) u = 0.2035, Model 3: (e) u = 0.19803, (f) u = 0.2035, Model 4: (g) u = 0.19803, (h) u = 0.2035.

pare our results with the values in Table 4.1. Thus, in Figure 4.11 we show the redshift z as a function of the radial coordinate. We can observe that z decreases outward and its value at the surface is less than the universal bound for interior solutions satisfying the DEC, namely $z_{bound} = 5.211$ [59].

Now, from the comparison of the value of density ratio for SMC X-1 reported in [99] being $\tilde{\rho}(0)/\tilde{\rho}(R) \approx 1.4659$, with the values of the Table 4.2, we appreciate that Models 3 and 4 fit

Figure 4.5: $\tilde{P}_t(r)$ as a function of r for Model 1: (a) u = 0.19803, (b) u = 0.2035, Model 2: (c) u = 0.19803, (d) u = 0.2035, Model 3: (e) u = 0.19803, (f) u = 0.2035, Model 4: (g) u = 0.19803, (h) u = 0.2035.

Model	$\rho(0)/\rho(R)$
Model 1 ($a_2 = 0.53$, $a_3 = 0.57$)	2.62443
Model 2 ($a_2 = 2.7$, $a_3 = 1.6$)	1.84825
Model 3 ($a_2 = 0.8$, $a_3 = 0.2$)	1.43124
Model 4 ($a_2 = 1.1$, $a_3 = 0.39$)	1.53133

Table 4.2: Estimated values of the density ratio for SMC X-1 (u = 0.19803).

accurately to SMC X-1. In the same way, $\tilde{\rho}(0)/\tilde{\rho}(R) \approx 1.915$ for Cen X-3 as appears in [101],

so the Models 2, 3 and 4 are suitable candidates to describe this compact objects.
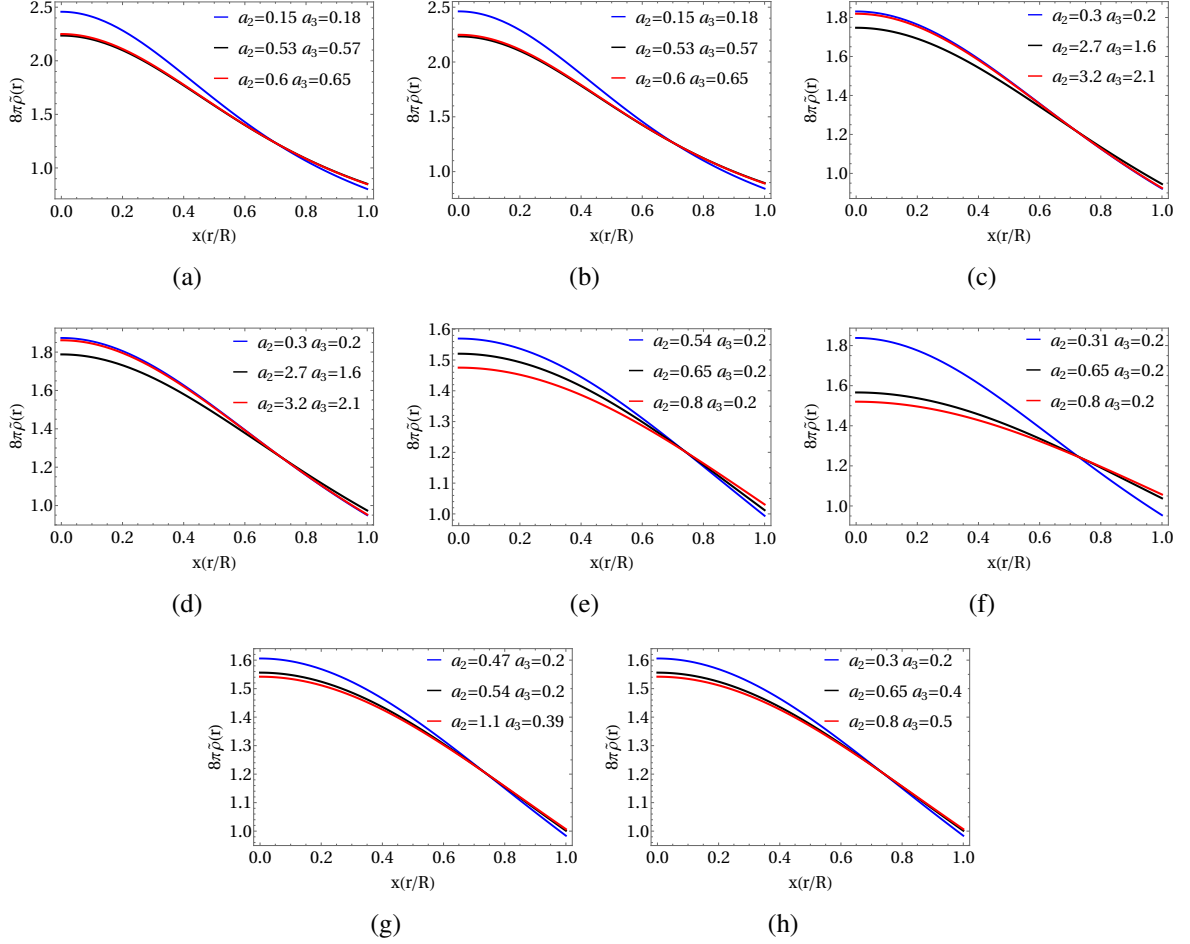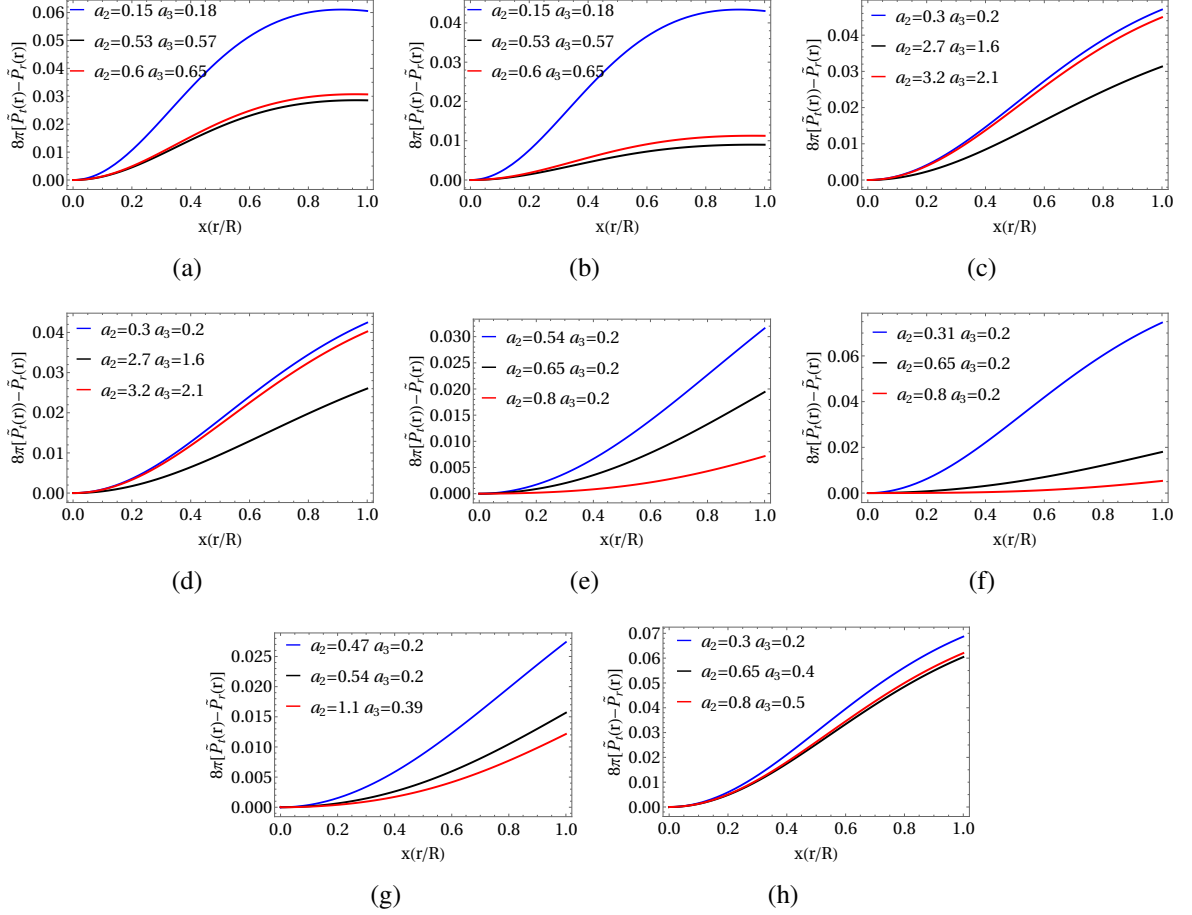
Figure 4.6: $\tilde{P}_t(r) - \tilde{P}_r(r)$ as a function of r for Model 1: (a) u = 0.19803, (b) u = 0.2035, Model 2: (c) u = 0.19803, (d) u = 0.2035, Model 3: (e) u = 0.19803, (f) u = 0.2035, Model 4: (g) u = 0.19803, (h) u = 0.2035.

Model	$\rho(0)/\rho(R)$
Model 1 ($a_2 = 0.53$, $a_3 = 0.57$)	2.49405
Model 2 ($a_2 = 0.3$, $a_3 = 0.2$)	1.97267
Model 3 ($a_2 = 0.31$, $a_3 = 0.2$)	1.92661
Model 4 ($a_2 = 0.8$, $a_3 = 0.5$)	1.92086

Table 4.3: Estimated values of the density ratio for Cen X-3 (u = 0.2035).

In summary, Models 3 and 4 might be considered as suitable solutions describing SMC X-1,
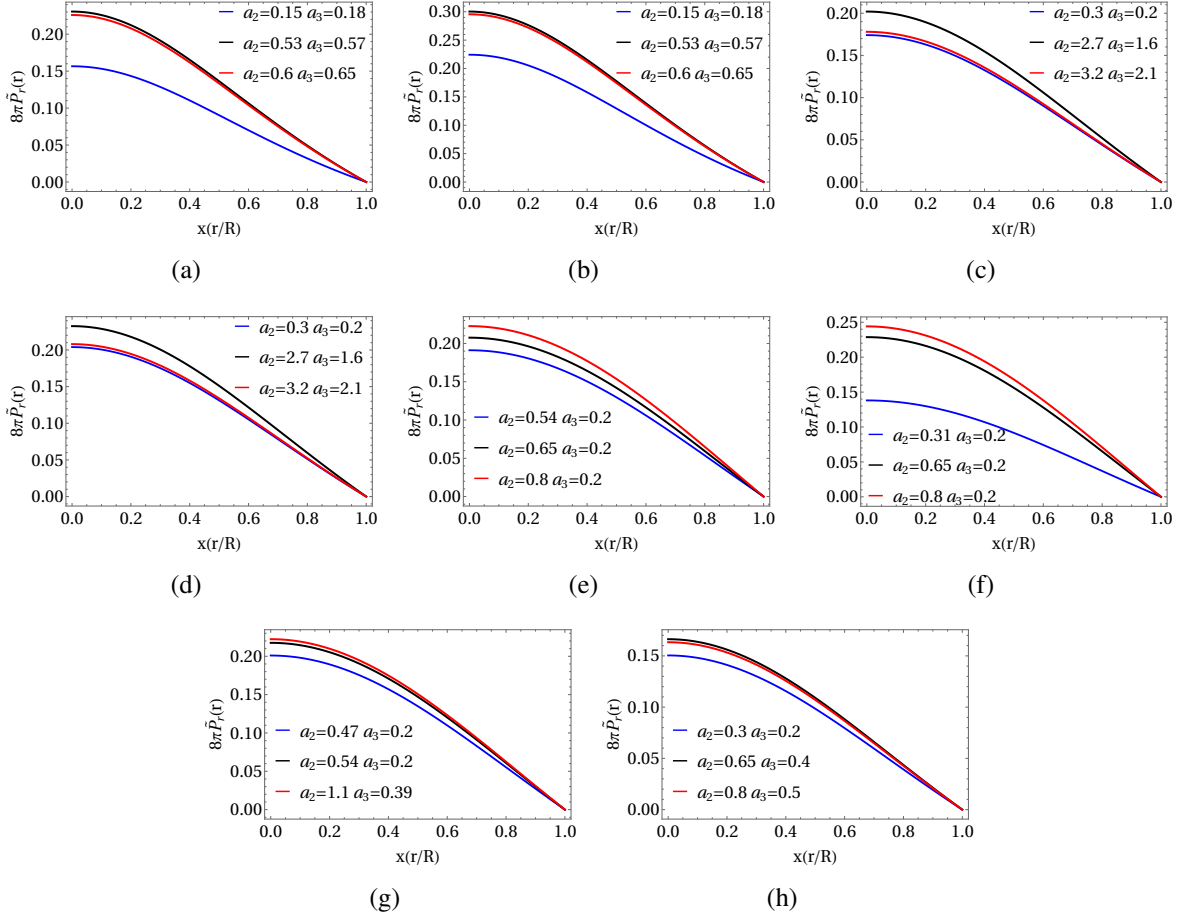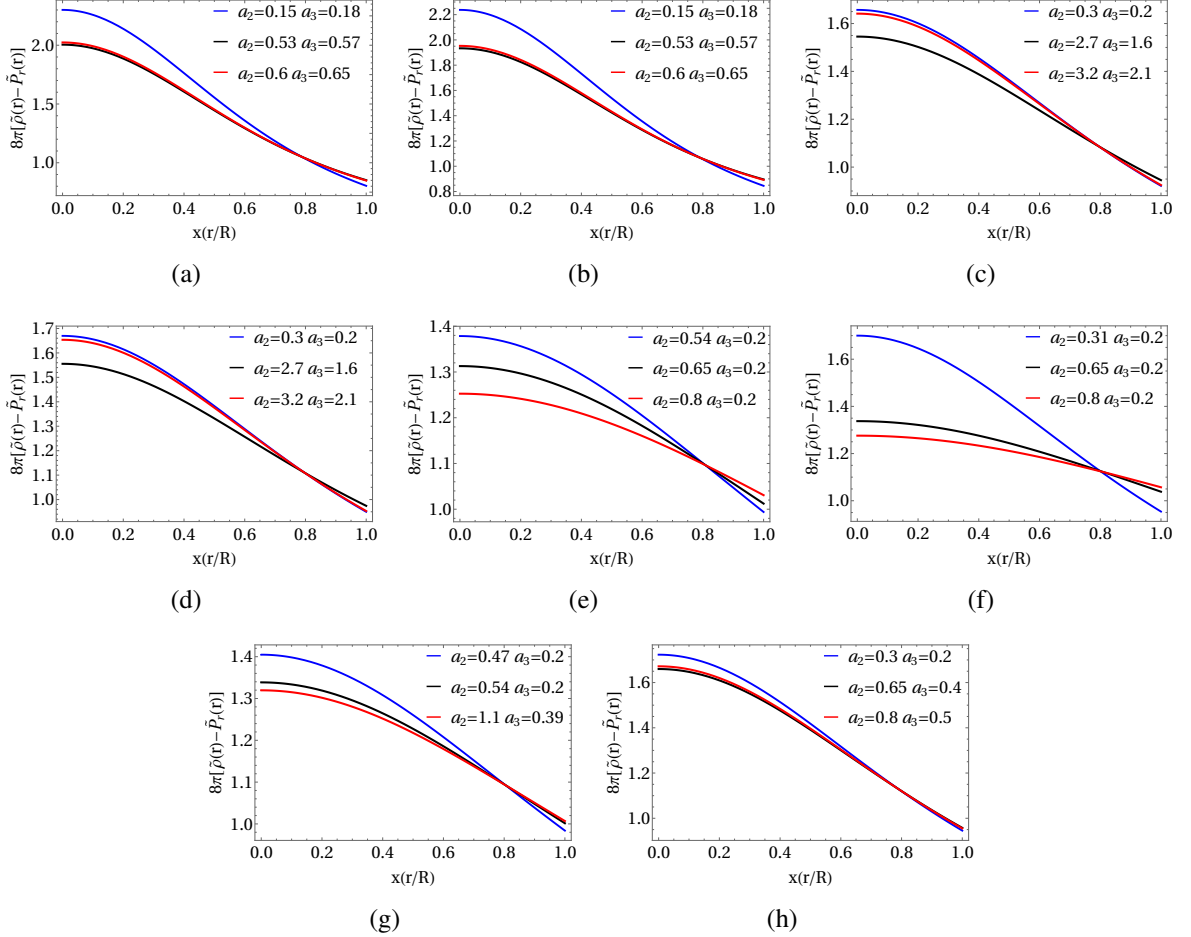
Figure 4.7: $\tilde{\rho}(r) - \tilde{P}_r(r)$ as a function of r for Model 1: (a) u = 0.19803, (b) u = 0.2035, Model 2: (c) u = 0.19803, (d) u = 0.2035, Model 3: (e) u = 0.19803, (f) u = 0.2035, Model 4: (g) u = 0.19803, (h) u = 0.2035.

while models 2, 3 and 4 are the solutions for Cen X-3.

4.5 Stability analysis

In this section we analyze the stability of models in the framework of gravitational cracking. In other words, we analyze the behavior of the perturbed total radial forces (3.55), (3.70), (3.84)
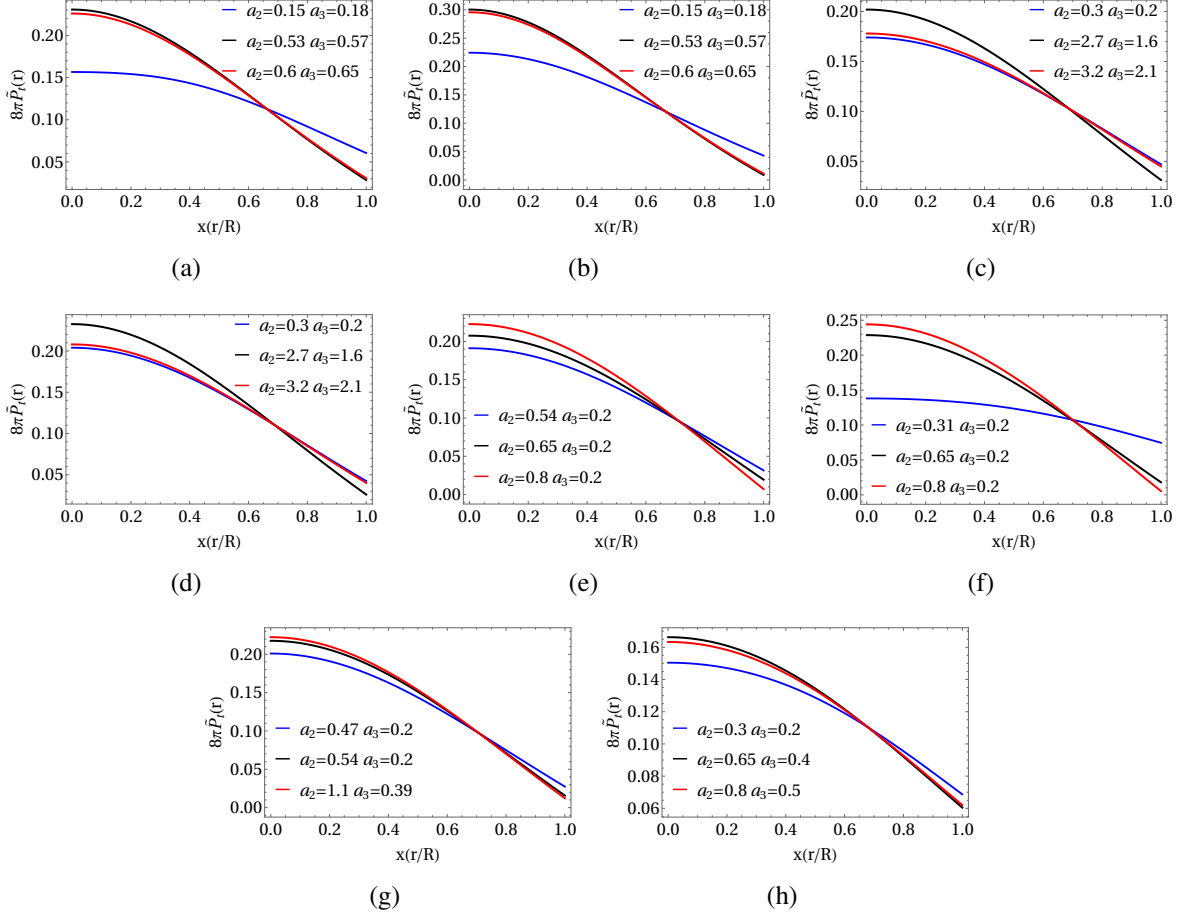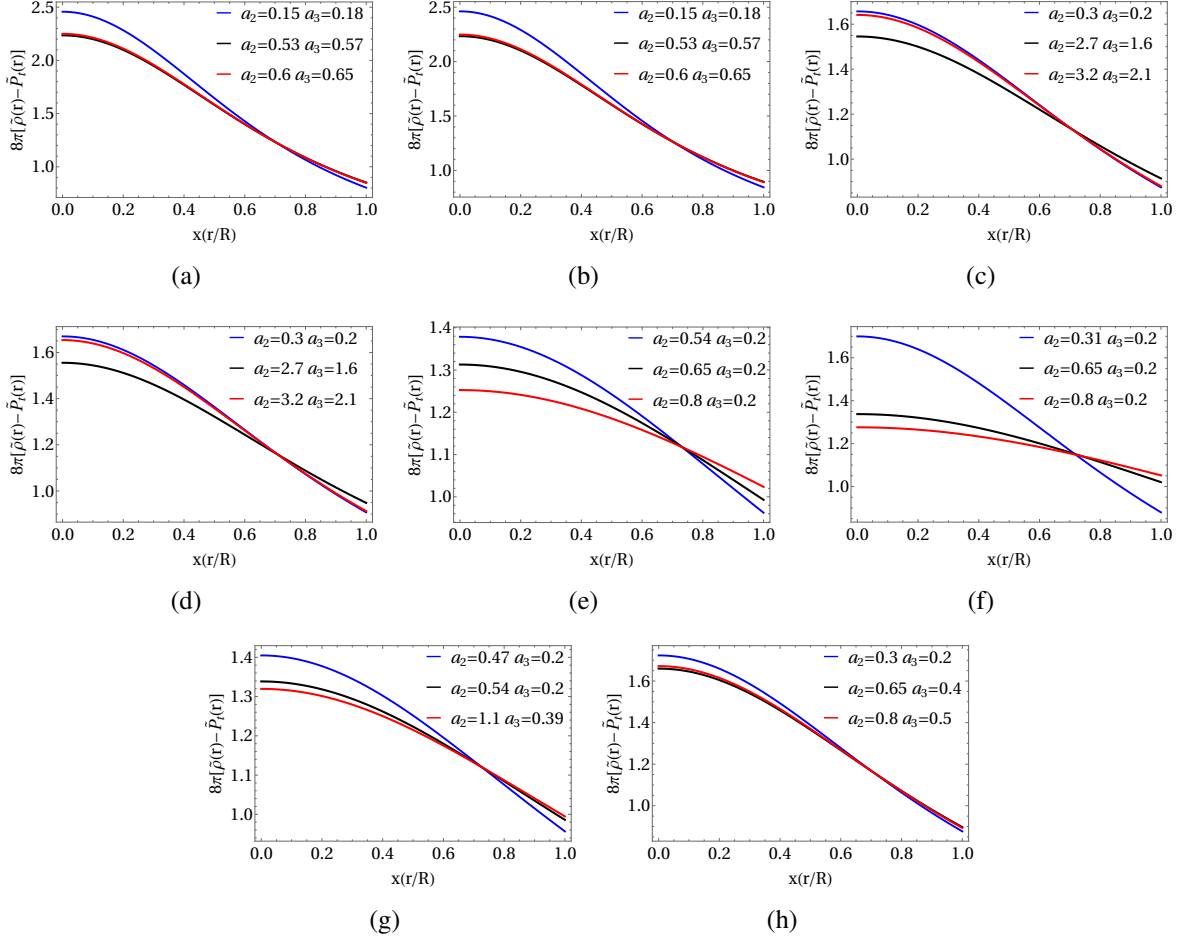
Figure 4.8: $\tilde{\rho}(r) - \tilde{P}_t(r)$ as a function of r for Model 1: (a) u = 0.19803, (b) u = 0.2035, Model 2: (c) u = 0.19803, (d) u = 0.2035, Model 3: (e) u = 0.19803, (f) u = 0.2035, Model 4: (g) u = 0.19803, (h) u = 0.2035.

and (3.98) to find the existence of any fracture (cracking and/or overturning) inside the fluid. We plot $\tilde{\mathcal{R}}$ as a function of x, for different values of Γ, α and β in order to explore the stability of each model.
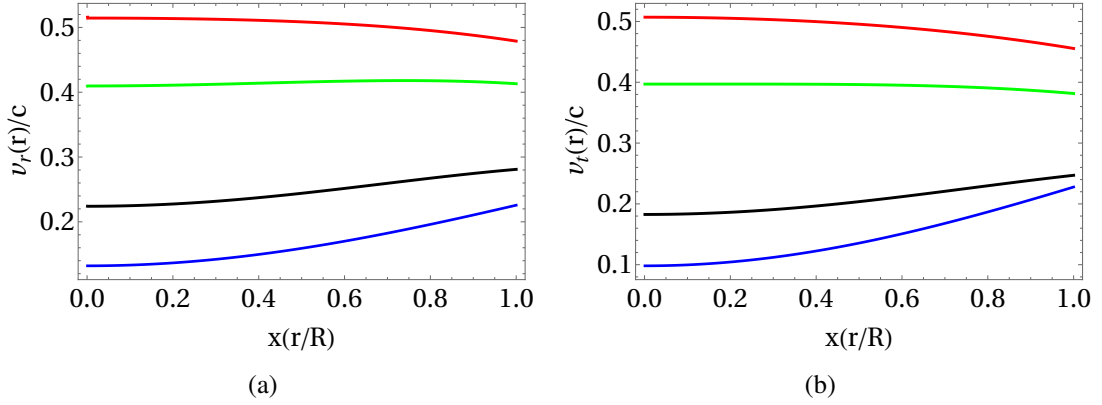
Figure 4.9: Sound velocities as a function of r for compactness factor $u = 0.19803$: (a) Radial velocity v_r and (b) Tangential velocity v_t. Models 1, 2, 3 and 4 are identified with blue, black, red and green line respectively.
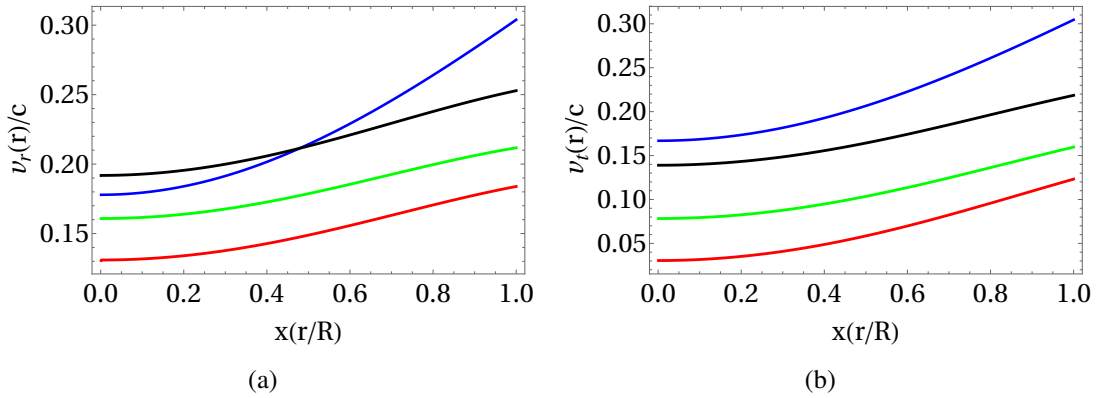
Figure 4.10: Sound velocities as a function of r for compactness factor $u = 0.2035$: (a) Radial velocity v_r and (b) Tangential v_t. Models 1, 2, 3 and 4 are identified with blue, black, red and green line respectively.

4.5.1 Cracking of Model 1

In this part we focus on the stability analysis for Model 1. For this purpose we study the behavior of (3.55). In the Figure 4.12 we show $\tilde{\mathcal{R}}$ as a function of x for different values of Γ. Note that there is overturning for positive Γ and cracking for negative Γ. Interestingly, the radius where cracking/overturning occurs coincide for all the values of Γ considered.
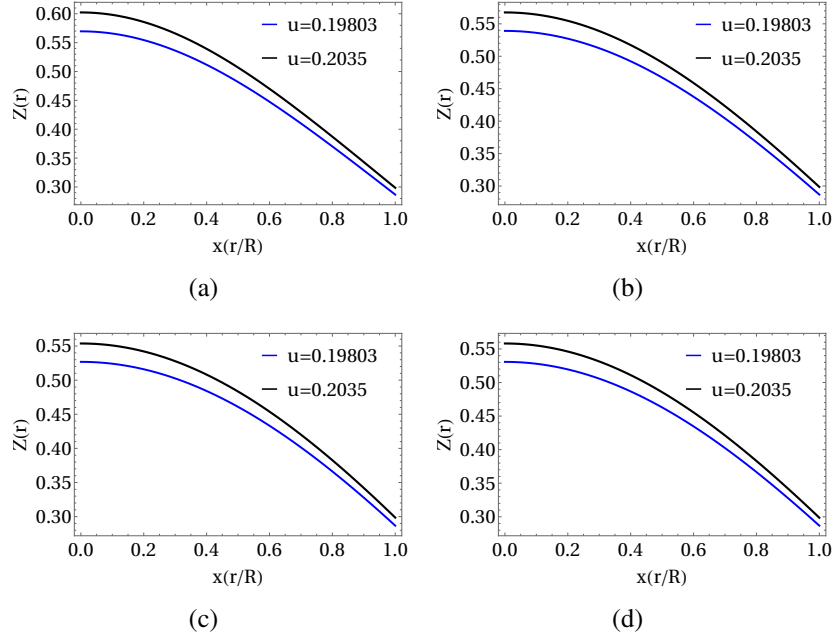
Figure 4.11: z for Model 1 (a) Model 2 (b) Model 3 (c) and Model 4 (d).
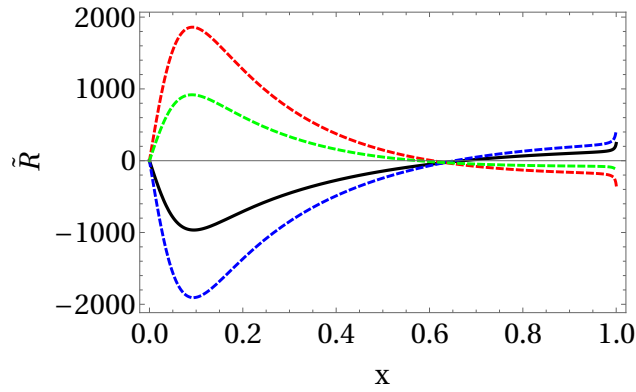
Figure 4.12: $\tilde{\mathcal{R}}$ as function of x (Model 1), for $a_3 = 0.57$, $\beta = 0.53$, $\alpha \approx 0.101$ ($u = 0.3322$); $\Gamma = 5$ (black line), $\Gamma = 2.5$ (blue line), $\Gamma = -2.5$ (red line) and $\Gamma = -5$ (green line).

The behavior of $\tilde{\mathcal{R}}$ as function of x respect to different values of β is shown in Figure 4.13, where we observe that as the value of β increases the stellar fluid distribution experiments overturning in outer regions.
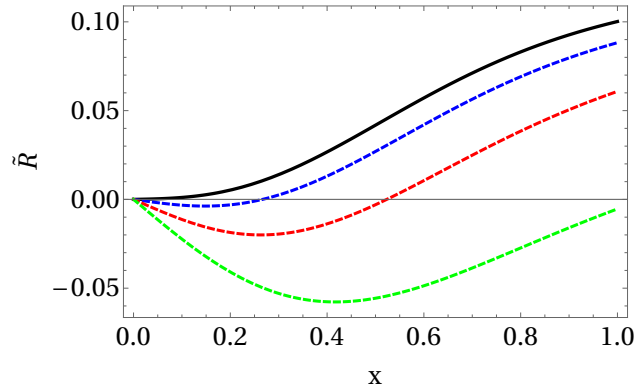
Figure 4.13: $\tilde{\mathcal{R}}$ as function of x (Model 1), for $a_3 = 0.57$, $\Gamma = -1.67$, $\alpha \approx 0.143169$ ($u = 0.19803$); $\beta = 0.53$ (black line), $\beta = 0.55$ (blue line), $\beta = 0.6$ (red line) and $\beta = 0.75$ (green line).

In Figure. 4.14, it is shown $\tilde{\mathcal{R}}$ as a function of x for different values of α. In this case it is noticeable that as the value of α decreases the fracture occurs in outer regions of fluid distribution; that is, such tendency is maintained for increasingly compact systems.
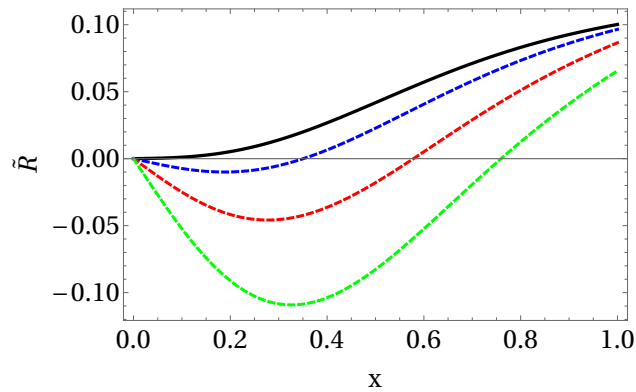
Figure 4.14: $\tilde{\mathcal{R}}$ as function of x (Model 1), for $a_3 = 0.57$, $\beta = 0.53$, $\Gamma = -1.67$; $\alpha \approx 1.43169$ ($u = 0.19803$) (black line), $\alpha \approx 1.38348$ ($u = 0.2035$) (blue line), $\alpha \approx 1.3$ ($u = 0.2132$) (red line) and $\alpha \approx 1.2$ ($u = 0.2252$) (green line).

4.5.2   Cracking of Model 2

In this subsection we analyze the stability of Model 2. In Figure 4.15 we show $\tilde{\mathcal{R}}$ (given by Eq.(3.70)) as a function of x for different values of Γ. We observe that fracture appears in the inner regions of the compact object as the value of Γ increases. Note that there is cracking and overturning for the same value $\Gamma = 0.9$ (green line), and that for the value of $\Gamma = 1.15$ (orange line) the model has stability. To be more precise, the system experiments a kind of transition between states with overturning and others with cracking due to the increasing of Γ.

It is worth emphasizing that, in this context, "stability" means that the system has absence of any fracture. To be specific, $\tilde{\mathcal{R}}$ does not change sing at any radius and that it does not have to be taken literally since the cracking approach only takes a "picture" of the tendency of radial force just after the system leaves equilibrium.
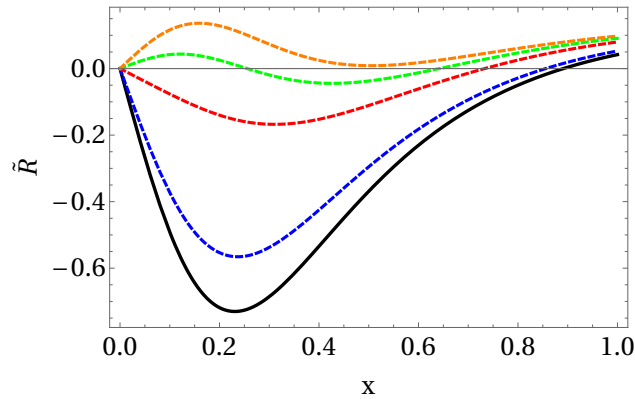
Figure 4.15: $\tilde{\mathcal{R}}$ as function of x (Model 2), for $a_2 = 0.3$, $A \approx -0.63793$, $\alpha \approx 0.13213$ ($u = 0.2035$), $\beta = 1.383$; $\Gamma = -0.9$ (black line), $\Gamma = -0.5$ (blue line), $\Gamma = 0.5$ (red line), $\Gamma = 0.9$ (green line) and $\Gamma = 1.15$ (orange line).

In Figure 4.16, plots of $\tilde{\mathcal{R}}$ as a function of x for different values of α (compactness factor) are shown. In this case the system goes from a configuration without fracture (orange line) to

situations where cracking and overturning appear (green and red lines) as the value of α increases. Also, we note that cracking appears in outer regions and overturning in inner regions as the value of compactness factor increases, and after the system becomes stable for upper compact objects.

Figure 4.16: $\tilde{\mathcal{R}}$ as function of x (Model 2), for $a_2 = 0.3$, $\Gamma = 1.0$, $\beta = 1.383$; $\alpha \approx 0.17678$ ($u = 0.25$) (black line), $\alpha \approx 0.14699$ ($u = 0.22$) (blue line), $\alpha \approx 0.13213$ ($u = 0.2035$) (red line), $\alpha \approx 0.12741$ ($u = 0.19803$) (green line) and $\alpha \approx 0.10463$ ($u = 0.17$) (orange line).

In Figure 4.17, we show $\tilde{\mathcal{R}}$ as a function of x for different values of β. In this case we note that the overturning point shifts to the center of the stellar object as the value of β reduces.

4.5.3 Cracking of Model 3

In this case we analyze the behavior of the disturbed total radial force (3.84). Thus, in Figure 4.18 we show $\tilde{\mathcal{R}}$ as a function of x for different values of Γ. We have that for positive Γ the system is stable, while for negative ones (blue and black line) the system experiments cracking (see Figure 4.18(a)), which moves to inner regions of fluid distribution as the value of Γ decreases (black and blue line) as can also be seen in Figure 4.18(b).
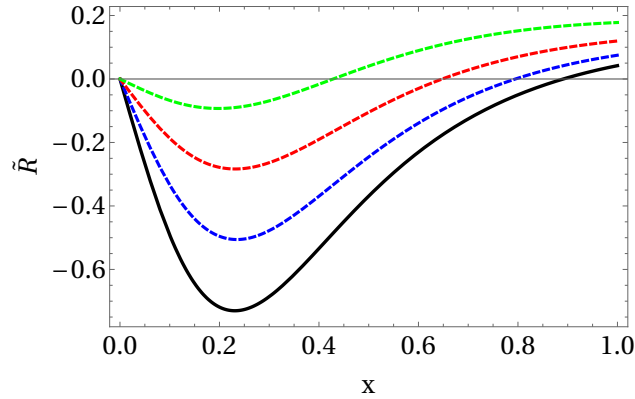
Figure 4.17: $\tilde{\mathcal{R}}$ as function of x (Model 2), for $a_2 = 0.3$, $A \approx -0.63793$, $\alpha = 0.13213$ ($u = 0.2035$), $\Gamma = -0.9$; $\beta = 1.38348$ (black line), $\beta = 1.2$ (blue line), $\beta = 1.0$ (red line) and $\beta = 0.8$ (green line).

(a)

(b)

Figure 4.18: $\tilde{\mathcal{R}}$ as function of x (Model 3), for $a_2 = 0.8$, $\alpha = 0.0893$ ($u = 0.19803$), $\beta = 0.2$; (a) $\Gamma = -12.0$ (black line), $\Gamma = -10.5$ (blue line), $\Gamma = 10.5$ (red line) and $\Gamma = 12.0$ (green line), (b) $\Gamma = -12.0$ (black line), $\Gamma = -13.0$ (blue line), $\Gamma = -14.0$ (red line) and $\Gamma = -15.0$ (green line)

Also in Figure 4.19, we show $\tilde{\mathcal{R}}$ as a function of x for distinct values of α. In this case there is cracking for the value of $\alpha = 1.6$ and 1.9 (black and blue line), while for upper values, such as $\alpha = 2.4$ and 2.8 (red and green line), the system presents cracking and overturning for the same value of the compactness factor. Note that the system experiments cracking in inner

regions of the fluid distribution as the value of α increases. Also note that the curves coincide at a specific radial value.
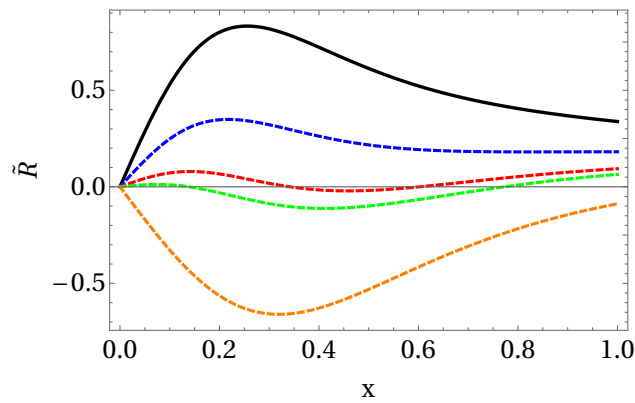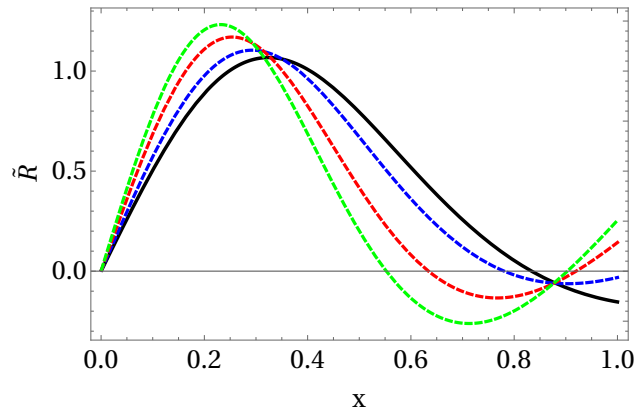

Figure 4.19: $\tilde{\mathcal{R}}$ as function of x (Model 3), for $a_2 = 0.8$, $\Gamma = -1.8$, $\beta = 0.2$; $\alpha \approx 1.6$ $(u = 0.4156)$ (black line), $\alpha \approx 1.91$ $(u = 0.42)$ (blue line), $\alpha \approx 2.4$ $(u = 0.4248)$ (red line) and $\alpha \approx 2.8$ $(u = 0.4275)$ (green line).

In Figure 4.20, curves of $\tilde{\mathcal{R}}$ as a function of x for different values of β are shown. In this case the fracture point moves to inner regions of the fluid as the value of β decreases. Also, we have that for the values of $\beta = 0.2$ and 1.2 (black and blue lines) the model experiments stability.
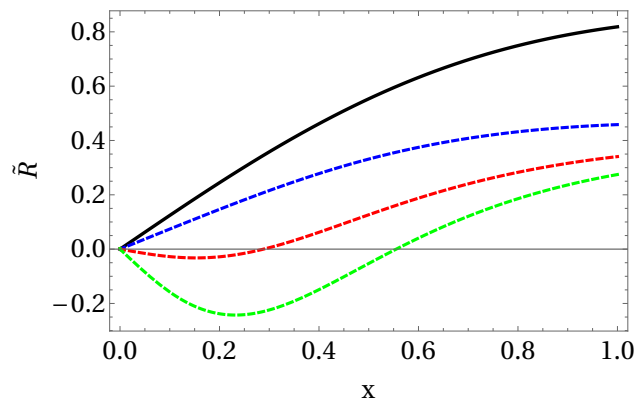
Figure 4.20: $\tilde{\mathcal{R}}$ as function of x (Model 3), for $a_2 = 0.8$, $\Gamma = -1.9$, $\alpha = 0.0893$ $(u = 0.19803)$; $\beta = 0.2$ (black line), $\beta = 1.2$ (blue line), $\beta = 1.9$ (red line) and $\beta = 2.5$ (green line).

4.5.4 Cracking of Model 4

In this part we analyze the stability of Model 4, for which we plot the perturbed total radial force (3.98) as function of x. Thus, in Figure 4.21, we show $\tilde{\mathcal{R}}$ as a function of x for distinct values of Γ. Observe that for the positive values of Γ the model is stable (red and green line), while that for $\Gamma = -10.0$ (black line) the system presents cracking (see Figure 4.21(a)), which moves to the inner regions of the stellar fluid distribution as the value of Γ decreases (see Figure 4.21(b)).
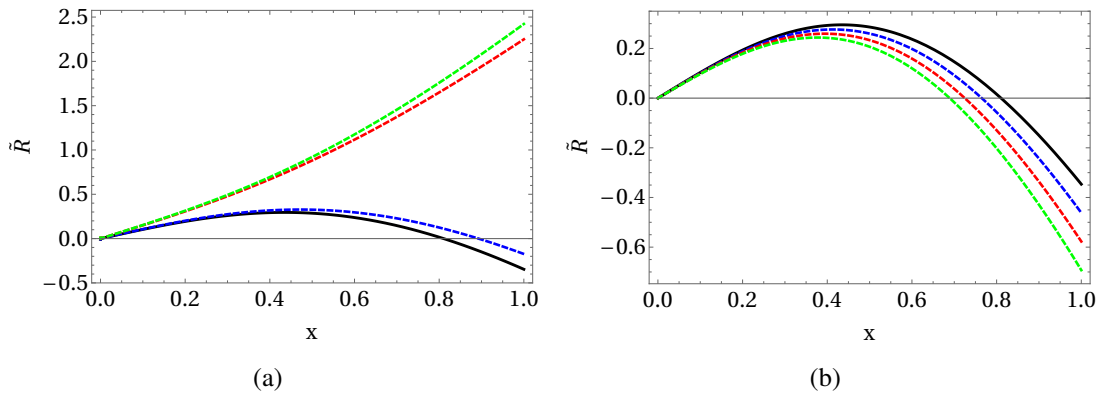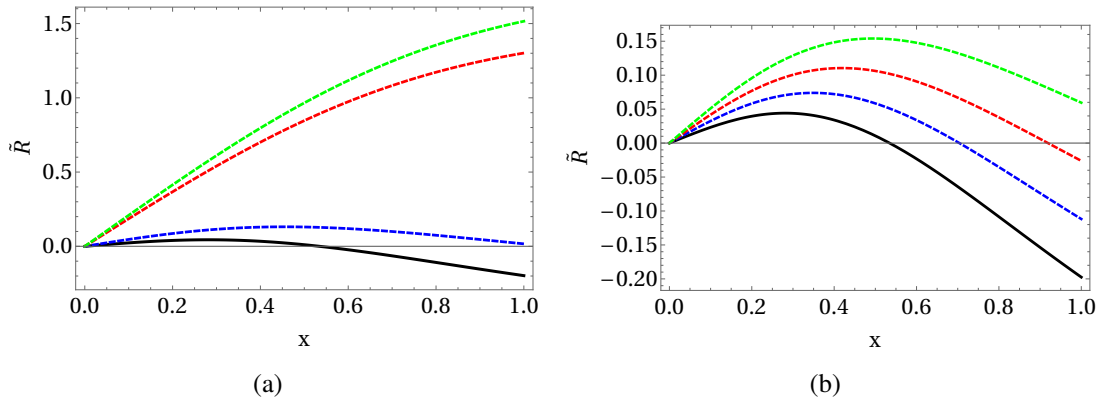

Figure 4.21: $\tilde{\mathcal{R}}$ as function of x (Model 4), for $a_2 = 0.8$, $\alpha \approx 0.12917$ ($u = 0.2035$), $\beta = 0.5$; (a) $\Gamma = -10.0$ (black line), $\Gamma = -7.5$ (blue line), $\Gamma = 7.5$ (red line) and $\Gamma = 10.0$ (green line), (b) $\Gamma = -10.0$ (black line), $\Gamma = -9.0$ (blue line), $\Gamma = -8.0$ (red line) and $\Gamma = -7.0$ (green line).

In Figure 4.22, $\tilde{\mathcal{R}}$ as a function of x for different values of α is shown. In this case the cracking appears in the inner regions of the fluid distribution as the value of α increases. Also, it is noticeable that for $\alpha = 7.54$ and 9.47 (red and green line) the system experiments cracking and overturning for the same value of compactness parameter; specifically, the cracking appears in the inner regions and overturning in the outer regions of the stellar fluid distribution for more compact objects. Note that the overturning appears at the same radius.
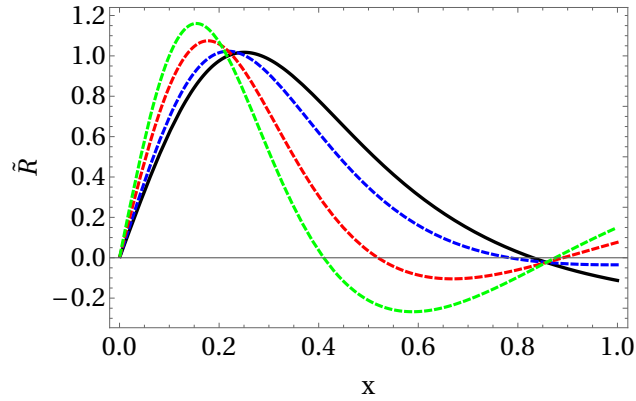
Figure 4.22: $\tilde{\mathcal{R}}$ as function of x (Model 4), for $a_2 = 0.8$, $\beta = 0.5$, $\Gamma = -1.8$; $\alpha \approx 4.51$ ($u = 0.4154$) (black line), $\alpha \approx 5.5$ ($u = 0.4178$) (blue line), $\alpha = 7.54$ ($u = 0.4206$) (red line) and $\alpha \approx 9.47$ ($u = 0.4222$) (green line).
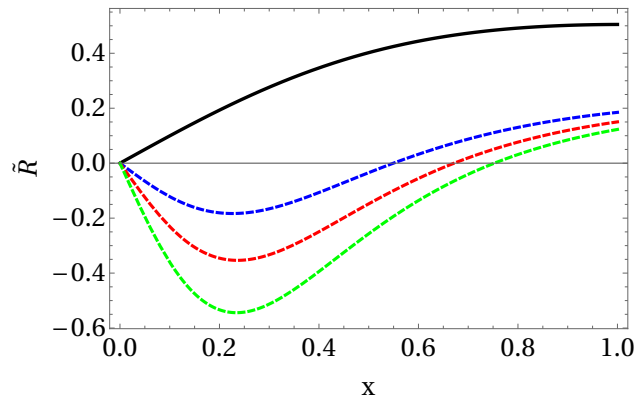
Figure 4.23: $\tilde{\mathcal{R}}$ as function of x (Model 4), for $a_2 = 0.8$, $\alpha = 0.12917$ ($u = 0.2035$), $\Gamma = -1.8$; $\beta = 0.5$ (black line), $\beta = 2.5$ (blue line), $\beta = 3.0$ (red line) and $\beta = 3.5$ (green line).

Finally, in Figure 4.23, we show $\tilde{\mathcal{R}}$ as function of x for different values of β. In this case the fracture appears in the outer regions of the fluid distribution as value of β increases, and that for the value of $\alpha = 0.5$ the model has stability.

Summarizing, we have observed the response of the models against perturbation just after the fluid distribution deviates from equilibrium, obtaining that all of them predict the existence

of fracture within the fluid of a compact object for certain sets of the parameters involved.

Chapter 5

Conclusions

In this work we extended four models of self-gravitating static spheres of isotropic fluid to anisotropic domains by Gravitational Decoupling through the Minimal Geometric Deformation using as supplementary condition, the complexity factor corresponding to a generalization obtained from the well–known Tolman IV interior solution. These new solutions fulfill the basic physical acceptability conditions; i) the metric functions are regular, and $g_{00}(0) = constant$ and $g^{11}(0) = 1$, ii) the density energy and pressures are regular at the origin and decrease monotonously outward, iii) causality conditions and iv) the solutions satisfy the dominant energy condition. Such conditions were tested for the compactness parameters of the systems SMC X-1 and Cen X-3. Also, these solutions are well behaved, but only for some parameters sets they can be considered as suitable models for the compact objects under consideration based on the density ratio. Precisely, Models 3 and 4 are more appropriated to describe SMC X-1 while Models 2, 3 and 4 can be used for Cen X-3.

Furthermore, we found that the four models presents fracture for certain settings of pa-

rameters. Indeed, these models presented exotic behavior for the total perturbed radial force having cracking and overturning, standing out a kind of transition between situations of cracking and overturning. Such transition for some configurations of parameters has intermediate states where the stellar fluid experiments cracking and overturning at the same time. In specific, for all models the strongest and deeper crackings occur for bigger values of the parameter α, which is directly related to the compactness factor of stellar compact object. Besides, most of the models trend to the "stability" as the value of Γ grows. This result is also observed for small values of α, which represents an interesting fact. Also, it is worth to mentioning, that for all models only overturning occurs inside the fluid when we study the behavior of $\tilde{\mathcal{R}}$ for different values of the parameter β. Such overturning point moves to outer regions of stellar fluid as the value of β increases.

Thus, we can evidence, theoretically, that the existence of any fracture inside a stellar fluid modeled by our models has a direct relation with fluctuations of the anisotropy and inhomogeneity of such fluid. The above follows from the fact that these quantities being present in the definition of the gravitational complexity factor for self-compact objects. Also, it is worth mentioning that the importance of this stability analysis results from the fact that the occurrence of cracking predicted by these models can be related with the possible origin of quakes in neutron stars, the collapse of super massive star or the ejection of outer shells in supernova event.

Additionally, it might be interesting to explore the possibility of generating new families following the same procedure presented in this work. Particularly such solutions can be based in other specific value of complexity factor, which can be a generalization of any other well-known solution or as also some specific function of radial coordinate. Also, these ideas can be

explored in the framework of the extended version of MGD.

Bibliography

[1] A. Einstein. Die grundlage der allgemeinen relativitätstheorie. *Annalen der Physik*, 354(7):769–822, 1916.

[2] Albert Einstein. Die Feldgleichungen der Gravitation. *Sitzungsberichte der Königlich Preußischen Akademie der Wissenschaften (Berlin*, pages 844–847, January 1915.

[3] Robert M Wald. *General relativity*. University of Chicago press, 2010.

[4] Karl Schwarzschild. Über das gravitationsfeld eines massenpunktes nach der einsteinschen theorie. *Sitzungsberichte der Königlich Preußischen Akademie der Wissenschaften (Berlin*, pages 189–196, 1916.

[5] Sean M Carroll. *Spacetime and geometry*. Cambridge University Press, 2019.

[6] Kip S Thorne, Charles W Misner, and John Archibald Wheeler. *Gravitation*. Freeman, 2000.

[7] Jiří Bičák. Selected solutions of einstein's field equations: Their role in general relativity and astrophysics. In Bernd G. Schmidt, editor, *Einstein's Field Equations and Their Physical Implications*, pages 1–126, Berlin, Heidelberg, 2000. Springer Berlin Heidelberg.

[8] Jerry B Griffiths and Jiří Podolskỳ. *Exact space-times in Einstein's general relativity.* Cambridge University Press, 2009.

[9] Hans Stephani, Dietrich Kramer, Malcolm MacCallum, Cornelius Hoenselaers, and Eduard Herlt. *Exact Solutions of Einstein's Field Equations.* Cambridge Monographs on Mathematical Physics. Cambridge University Press, 2 edition, 2003.

[10] Richard C Tolman. Static solutions of einstein's field equations for spheres of fluid. *Physical Review*, 55(4):364, 1939.

[11] Omair Zubairi, Alexis Romero, and Fridolin Weber. Static solutions of einstein's field equations for compact stellar objects. In *Journal of Physics: Conference Series*, volume 615, page 012003. IOP Publishing, 2015.

[12] MSR Delgaty and Kayll Lake. Physical acceptability of isolated, static, spherically symmetric, perfect fluid solutions of einstein's equations. *Computer Physics Communications*, 115(2-3):395–415, 1998.

[13] BV Ivanov. Analytical study of anisotropic compact star models. *The European Physical Journal C*, 77(11):1–12, 2017.

[14] PS Negi. Exact solutions of einstein's field equations. *International Journal of Theoretical Physics*, 45(9):1684–1702, 2006.

[15] MK Mak and T Harko. Anisotropic stars in general relativity. *Proceedings of the Royal Society of London. Series A: Mathematical, Physical and Engineering Sciences*, 459(2030):393–408, 2003.

[16] L. Herrera and N.O. Santos. Local anisotropy in self-gravitating systems. *Physics Reports*, 286(2):53 – 130, 1997.

[17] W Hillebrandt and KO Steinmetz. Anisotropic neutron star models-stability against radial and nonradial pulsations. *Astronomy and Astrophysics*, 53:283–287, 1976.

[18] L Herrera. Stability of the isotropic pressure condition. *Physical Review D*, 101(10):104024, 2020.

[19] Richard L Bowers and EPT Liang. Anisotropic spheres in general relativity. *The Astrophysical Journal*, 188:657, 1974.

[20] Petros S Florides. A new interior schwarzschild solution. *Proceedings of the Royal Society of London. A. Mathematical and Physical Sciences*, 337(1611):529–535, 1974.

[21] M Cosenza, L Herrera, M Esculpi, and L Witten. Some models of anisotropic spheres in general relativity. *Journal of Mathematical Physics*, 22(1):118–125, 1981.

[22] Kayll Lake. All static spherically symmetric perfect-fluid solutions of einstein's equations. *Physical Review D*, 67(10):104015, 2003.

[23] L Herrera, J Ospino, and A Di Prisco. All static spherically symmetric anisotropic solutions of einstein's equations. *Physical Review D*, 77(2):027502, 2008.

[24] Ernesto Contreras, Ernesto Fuenmayor, and Pedro Bargueño. All static spherically symmetric anisotropic solutions for general relativistic polytropes. *arXiv preprint arXiv:1905.05378*, 2019.

[25] Jorge Ovalle. Decoupling gravitational sources in general relativity: from perfect to anisotropic fluids. *Physical Review D*, 95(10):104019, 2017.

[26] Milko Estrada and Francisco Tello-Ortiz. A new family of analytical anisotropic solutions by gravitational decoupling. *The European Physical Journal Plus*, 133(11):1–15, 2018.

[27] Jorge Ovalle and Roberto Casadio. Gravitational decoupling. In *Beyond Einstein Gravity*, pages 95–112. Springer, 2020.

[28] Jorge Ovalle. Decoupling gravitational sources in general relativity: The extended case. *Physics Letters B*, 788:213–218, 2019.

[29] Ernesto Contreras and Pedro Bargueño. Extended gravitational decoupling in 2+ 1 dimensional space-times. *Classical and Quantum Gravity*, 36(21):215009, 2019.

[30] Pablo León and Adrián Sotomayor. Braneworld gravity under gravitational decoupling. *Fortschritte der Physik*, 67(12):1900077, 2019.

[31] Francisco X Linares Cedeño and Ernesto Contreras. Gravitational decoupling in cosmology. *Physics of the Dark Universe*, 28:100543, 2020.

[32] Francisco Tello-Ortiz. Minimally deformed anisotropic dark stars in the framework of gravitational decoupling. *The European Physical Journal C*, 80:1–15, 2020.

[33] J Ovalle, R Casadio, E Contreras, and A Sotomayor. Hairy black holes by gravitational decoupling. *Physics of the Dark Universe*, 31:100744, 2020.

[34] Jorge Ovalle, Roberto Casadio, Roldão da Rocha, Adrián Sotomayor, and Zdeněk Stuchlík. Black holes by gravitational decoupling. *The European Physical Journal C*, 78(11):1–11, 2018.

[35] Louis Bel. Inductions électromagnétique et gravitationnelle. In *Annales de l'institut Henri Poincaré*, volume 17, pages 37–57, 1961.

[36] L Herrera. New definition of complexity for self-gravitating fluid distributions: The spherically symmetric, static case. *Physical Review D*, 97(4):044010, 2018.

[37] Hermann Bondi. Massive spheres in general relativity. *Proceedings of the Royal Society of London. Series A. Mathematical and Physical Sciences*, 282(1390):303–317, 1964.

[38] S Chandrasekhar. Dynamical instability of gaseous masses approaching the schwarzschild limit in general relativity. *Physical Review Letters*, 12(4):114, 1964.

[39] S Chandrasekhar. Erratum: the dynamical instability of gaseous masses approaching the schwarzschild limit in general relativity. *The Astrophysical Journal*, 140:1342, 1964.

[40] S Chandrasekhar. A general variational principle governing the radial and the non-radial oscillations of gaseous masses. *VI. Ellipsoidal Figures of Equilibrium*, 1(2), 1960.

[41] L Herrera. Cracking of self-gravitating compact objects. *Physics Letters A*, 165(3):206–210, 1992.

[42] Alicia Di Prisco, Ernesto Fuenmayor, Luis Herrera, and Victor Varela. Tidal forces and fragmentation of self-gravitating compact objects. *Physics Letters A*, 195(1):23–26, 1994.

[43] Alicia Di Prisco, Luis Herrera, and Victor Varela. Cracking of homogeneous self-gravitating compact objects induced by fluctuations of local anisotropy. *General Relativity and Gravitation*, 29(10):1239–1256, 1997.

[44] Sean M Carroll. An introduction to general relativity: spacetime and geometry. *Addison Wesley*, 101:102, 2004.

[45] Bernard Schutz. *A first course in general relativity*. Cambridge university press, 2009.

[46] Rudolf Kippenhahn, Alfred Weigert, and Achim Weiss. *Stellar structure and evolution*, volume 192. Springer, 1990.

[47] Max Wyman. Radially symmetric distributions of matter. *Physical Review*, 75(12):1930, 1949.

[48] MC Durgapal. A class of new exact solutions in general relativity. *Journal of Physics A: Mathematical and General*, 15(8):2637, 1982.

[49] H Heintzmann. New exact static solutions of einsteins field equations. *Zeitschrift für Physik*, 228(4):489–493, 1969.

[50] John M Lee. *Riemannian manifolds: an introduction to curvature*, volume 176. Springer Science & Business Media, 2006.

[51] George David Birkhoff and Rudolph Ernest Langer. *Relativity and modern physics*, volume 1. Harvard University Press Cambridge, 1923.

[52] Georges Darmois. Mémorial des sciences mathématiques. *Fascicule XXV (Gauthier-Villars, Paris, 1927)*, 1927.

[53] WB Bonnor and PA Vickers. Junction conditions in general relativity. *General Relativity and Gravitation*, 13(1):29–36, 1981.

[54] Georges Lemaître. L'univers en expansion. In *Annales de la Société scientifique de Bruxelles*, volume 53, page 51, 1933.

[55] M Ruderman. Pulsars: structure and dynamics. *Annual Review of Astronomy and Astrophysics*, 10(1):427–476, 1972.

[56] Luis Herrera and Nilton O Santos. Local anisotropy in self-gravitating systems. *Physics Reports*, 286(2):53–130, 1997.

[57] Steven Carlip. The einstein field equations. In *General Relativity*, pages 52–58. Oxford University Press, 2019.

[58] Norman K Glendenning. *Compact stars: Nuclear physics, particle physics and general relativity*. Springer Science & Business Media, 2012.

[59] Boiko V Ivanov. Maximum bounds on the surface redshift of anisotropic stars. *Physical Review D*, 65(10):104011, 2002.

[60] J Ovalle. Searching exact solutions for compact stars in braneworld: a conjecture. *Modern Physics Letters A*, 23(38):3247–3263, 2008.

[61] J Ovalle. Braneworld stars: anisotropy minimally projected onto the brane. In *Gravitation and Astrophysics*, pages 173–182. World Scientific, 2010.

[62] Lisa Randall and Raman Sundrum. Large mass hierarchy from a small extra dimension. *Physical review letters*, 83(17):3370, 1999.

[63] Lisa Randall and Raman Sundrum. An alternative to compactification. *Physical Review Letters*, 83(23):4690, 1999.

[64] Roberto Casadio, Jorge Ovalle, and Roldao Da Rocha. The minimal geometric deformation approach extended. *Classical and Quantum Gravity*, 32(21):215020, 2015.

[65] Jorge Ovalle. Extending the geometric deformation: New black hole solutions. In *International Journal of Modern Physics: Conference Series*, volume 41, page 1660132. World Scientific, 2016.

[66] J Ovalle and F Linares. Tolman iv solution in the randall-sundrum braneworld. *Physical Review D*, 88(10):104026, 2013.

[67] Alfonso García-Parrado Gómez-Lobo. Dynamical laws of superenergy in general relativity. *Classical and quantum gravity*, 25(1):015006, 2007.

[68] R Casadio, E Contreras, J Ovalle, A Sotomayor, and Z Stuchlik. Isotropization and change of complexity by gravitational decoupling. *The European Physical Journal C*, 79(10):1–8, 2019.

[69] Hans A Buchdahl. General relativistic fluid spheres. *Physical Review*, 116(4):1027, 1959.

[70] L Herrera, J Jiménez, and GJ Ruggeri. Evolution of radiating fluid spheres in general relativity. *Physical Review D*, 22(10):2305, 1980.

[71] L Herrera and L Nunez. Modeling'hydrodynamic phase transitions' in a radiating spherically symmetric distribution of matter. *The Astrophysical Journal*, 339:339–353, 1989.

[72] Luis Herrera and LA Nunez. Luminosity profiles and the evolution of shock waves in general relativistic radiating spheres. Technical report, International Centre for Theoretical Physics, 1989.

[73] José P Mimoso, Morgan Le Delliou, and Filipe C Mena. Separating expansion from contraction in spherically symmetric models with a perfect fluid: Generalization of the

tolman-oppenheimer-volkoff condition and application to models with a cosmological constant. *Physical Review D*, 81(12):123514, 2010.

[74] Morgan Le Delliou, José P Mimoso, Filipe C Mena, Michele Fontanini, Daniel C Guariento, and Elcio Abdalla. Separating expansion and collapse in general fluid models with heat flux. *Physical Review D*, 88(2):027301, 2013.

[75] José P Mimoso, Morgan Le Delliou, and Filipe C Mena. Local conditions separating expansion from collapse in spherically symmetric models with anisotropic pressures. *Physical Review D*, 88(4):043501, 2013.

[76] Lucia M Franco, Bennett Link, and Richard I Epstein. Quaking neutron stars. *The Astrophysical Journal*, 543(2):987, 2000.

[77] Bennett Link, Lucia M Franco, and Richard I Epstein. Starquake-induced magnetic field and torque evolution in neutron stars. *The Astrophysical Journal*, 508(2):838, 1998.

[78] Christopher Thompson and Robert C Duncan. The soft gamma repeaters as very strongly magnetized neutron stars. ii. quiescent neutrino, x-ray, and alfven wave emission. *The Astrophysical Journal*, 473(1):322, 1996.

[79] Christopher Thompson and Omer Blaes. Magnetohydrodynamics in the extreme relativistic limit. *Physical Review D*, 57(6):3219, 1998.

[80] R Chan. L. herrera l and no santos. *Mon. Not. R. Astron. Soc*, 265:533, 1993.

[81] James C Kemp, John B Swedlund, JD Landstreet, and JRP Angel. Discovery of circularly polarized light from a white dwarf. *The Astrophysical Journal*, 161:L77, 1970.

[82] Angela Putney. Three new magnetic white dwarf stars. *The Astrophysical Journal Letters*, 451(2):L67, 1995.

[83] R González Felipe, E López Fune, D Manreza Paret, and A Pérez Martínez. Magnetized strangelets at finite temperature. *Journal of Physics G: Nuclear and Particle Physics*, 39(4):045006, 2012.

[84] Diana Alvear Terrero, Samantha López Pérez, Daryel Manreza Paret, Aurora Pérez Martínez, and Gretel Quintero Angulo. Observables of spheroidal magnetized strange stars. *arXiv preprint arXiv:2010.06514*, 2020.

[85] Masud Chaichian, SS Masood, Claus Montonen, A Perez Martinez, and H Pérez Rojas. Quantum magnetic collapse. *Physical Review Letters*, 84(23):5261, 2000.

[86] A Pérez Martínez, H Pérez Rojas, and HJ Mosquera Cuesta. Magnetic collapse of a neutron gas: Can magnetars indeed be formed? *The European Physical Journal C-Particles and Fields*, 29(1):111–123, 2003.

[87] A Perez Martinez, H Perez Rojas, and HJ Mosquera Cuesta. Anisotropic pressures in very dense magnetized matter. *International Journal of Modern Physics D*, 17(11):2107–2123, 2008.

[88] Efrain J Ferrer, Vivian de La Incera, Jason P Keith, Israel Portillo, and Paul L Springsteen. Equation of state of a dense and magnetized fermion system. *Physical Review C*, 82(6):065802, 2010.

[89] Michael Strickland, Veronica Dexheimer, and Debora P Menezes. Bulk properties of a fermi gas in a magnetic field. *Physical Review D*, 86(12):125032, 2012.

[90] N Andersson, GL Comer, and K Glampedakis. How viscous is a superfluid neutron star core? *Nuclear Physics A*, 763:212–229, 2005.

[91] Basil A Sa'd, Igor A Shovkovy, and Dirk H Rischke. Bulk viscosity of strange quark matter: Urca versus nonleptonic processes. *Physical Review D*, 75(12):125004, 2007.

[92] Mark G Alford and Andreas Schmitt. Bulk viscosity in 2sc and cfl quark matter. In *AIP Conference Proceedings*, volume 964, pages 256–263. American Institute of Physics, 2007.

[93] Alessandro Drago, A Lavagno, and Giuseppe Pagliara. Bulk viscosity in hybrid stars. *Physical Review D*, 71(10):103004, 2005.

[94] PB Jones. Bulk viscosity of neutron-star matter. *Physical Review D*, 64(8):084003, 2001.

[95] ENE Van Dalen and AEL Dieperink. Bulk viscosity in neutron stars from hyperons. *Physical Review C*, 69(2):025802, 2004.

[96] Hui Dong, Nan Su, and Qun Wang. Bulk viscosity in nuclear and quark matter. *Journal of Physics G: Nuclear and Particle Physics*, 34(8):S643, 2007.

[97] Curt Cutler and Lee Lindblom. The effect of viscosity on neutron star oscillations. *The Astrophysical Journal*, 314:234–241, 1987.

[98] Meredith L Rawls, Jerome A Orosz, Jeffrey E McClintock, Manuel AP Torres, Charles D Bailyn, and Michelle M Buxton. Refined neutron star mass determinations for six eclipsing x-ray pulsar binaries. *The Astrophysical Journal*, 730(1):25, 2011.

[99] SK Maurya, Ayan Banerjee, and YK Gupta. Exact solution of anisotropic compact stars via mass function. *Astrophysics and Space Science*, 363(10):1–9, 2018.

[100] VA Torres-Sánchez and Ernesto Contreras. Anisotropic neutron stars by gravitational decoupling. *The European Physical Journal C*, 79(10):1–8, 2019.

[101] AK Prasad, J Kumar, SK Maurya, and B Dayanandan. Relativistic model for anisotropic compact stars using karmarkar condition. *Astrophysics and Space Science*, 364(4):1–12, 2019.

INDEX OF ANNEXES

Annex A

Einstein's tensor for Static and Spherical symmetric spacetime

1.1 Connections

We obtain the connections (Christoffel symbol of the second kind) corresponding to the metric (2.8) through the definition (2.6), resulting that there are only nine non null connections

$$
\begin{aligned}
\Gamma^1_{11} &= \frac{1}{2}\lambda', \\
\Gamma^1_{00} &= \frac{1}{2}\nu' e^{\nu-\lambda}, \\
\Gamma^1_{22} &= -re^{-\lambda}, \\
\Gamma^1_{33} &= -re^{-\lambda}\sin^2\theta, \\
\Gamma^2_{33} &= -\sin\theta\cos\theta, \\
\Gamma^0_{01} &= \frac{1}{2}\nu', \\
\Gamma^2_{21} &= \Gamma^3_{31} = \frac{1}{r}, \\
\Gamma^3_{32} &= \cot\theta.
\end{aligned}
$$

1.2 Ricci's tensor components

So with the nine non null connections we can calculate the only non zero Ricci's tensor components with the help of (2.3) and (2.5) obtaining

$$
\begin{aligned}
R_{00} &= \partial_\lambda \Gamma^\lambda_{00} - \partial_0 \Gamma^\lambda_{\lambda 0} + \Gamma^\lambda_{\lambda \sigma} \Gamma^\sigma_{00} - \Gamma^\lambda_{\sigma 0} \Gamma^\sigma_{\lambda 0} \\
&= \partial_1 \Gamma^1_{00} + \Gamma^\lambda_{\lambda 1} \Gamma^1_{00} - \Gamma^0_{\sigma 0} \Gamma^\sigma_{00} - \Gamma^1_{\sigma 0} \Gamma^\sigma_{10} - \Gamma^2_{\sigma 0} \Gamma^\sigma_{20} - \Gamma^3_{\sigma 0} \Gamma^\sigma_{30} \\
&= \partial_1 \Gamma^1_{00} + \Gamma^0_{10} \Gamma^1_{00} + \Gamma^1_{11} \Gamma^1_{00} + \Gamma^2_{21} \Gamma^1_{00} + \Gamma^3_{31} \Gamma^1_{00} - \Gamma^0_{10} \Gamma^1_{00} - \Gamma^1_{00} \Gamma^0_{10} \\
&= \partial_1 \Gamma^1_{00} + \Gamma^1_{11} \Gamma^1_{00} + \Gamma^2_{21} \Gamma^1_{00} + \Gamma^3_{31} \Gamma^1_{00} - \Gamma^1_{00} \Gamma^0_{10} \\
&= \frac{\partial}{\partial r}\left(\frac{1}{2}\nu' e^{\nu-\lambda}\right) + \frac{1}{4}\lambda'\nu' e^{\nu-\lambda} + \frac{1}{2r}\nu' e^{\nu-\lambda} + \frac{1}{2r}\nu' e^{\nu-\lambda} - \frac{1}{4}\nu'^2 e^{\nu-\lambda} \\
&= e^{\nu-\lambda}\left(\frac{1}{2}\nu'' + \frac{1}{4}\nu'^2 - \frac{1}{4}\nu'\lambda' + \frac{\nu'}{r}\right),
\end{aligned}
$$

$$
\begin{aligned}
R_{11} &= \partial_\lambda \Gamma^\lambda_{11} - \partial_1 \Gamma^\lambda_{\lambda 1} + \Gamma^\lambda_{\lambda \sigma} \Gamma^\sigma_{11} - \Gamma^\lambda_{\sigma 1} \Gamma^\sigma_{\lambda 1} \\
&= \partial_1 \Gamma^1_{11} - \partial_1 \Gamma^0_{01} - \partial_1 \Gamma^1_{11} - \partial_1 \Gamma^2_{21} - \partial_1 \Gamma^3_{31} + \Gamma^\lambda_{\lambda 1} \Gamma^1_{11} - \Gamma^0_{\sigma 1} \Gamma^\sigma_{01} - \Gamma^1_{\sigma 1} \Gamma^\sigma_{11} \\
&\quad - \Gamma^2_{\sigma 1} \Gamma^\sigma_{21} - \Gamma^3_{\sigma 1} \Gamma^\sigma_{31} \\
&= -\partial_1 \Gamma^0_{01} - \partial_1 \Gamma^2_{21} - \partial_1 \Gamma^3_{31} + \Gamma^0_{01} \Gamma^1_{11} + \Gamma^1_{11} \Gamma^1_{11} + \Gamma^2_{21} \Gamma^1_{11} + \Gamma^3_{31} \Gamma^1_{11} - \Gamma^0_{01} \Gamma^0_{01} \\
&\quad - \Gamma^1_{11} \Gamma^1_{11} - \Gamma^2_{21} \Gamma^2_{21} - \Gamma^3_{31} \Gamma^3_{31} \\
&= -\partial_1 \Gamma^0_{01} - \partial_1 \Gamma^2_{21} - \partial_1 \Gamma^3_{31} + \Gamma^0_{01} \Gamma^1_{11} + \Gamma^2_{21} \Gamma^1_{11} + \Gamma^3_{31} \Gamma^1_{11} - \Gamma^0_{01} \Gamma^0_{01} - \Gamma^2_{21} \Gamma^2_{21} \\
&\quad - \Gamma^3_{31} \Gamma^3_{31} \\
&= -\frac{\partial}{\partial r}\left(\frac{1}{2}\nu'\right) - \frac{\partial}{\partial r}\left(\frac{1}{r}\right) - \frac{\partial}{\partial r}\left(\frac{1}{r}\right) + \frac{1}{4}\nu'\lambda' + \frac{1}{2r}\lambda' + \frac{1}{2r}\lambda' - \frac{1}{4}\nu'^2 \\
&\quad - \frac{1}{r^2} - \frac{1}{r^2} \\
&= -\frac{\nu''}{2} + \frac{1}{4}\lambda'\nu' - \frac{1}{4}\nu'^2 + \frac{\lambda'}{r},
\end{aligned}
$$

$$
\begin{aligned}
R_{22} &= \partial_\lambda \Gamma^\lambda_{22} - \partial_2 \Gamma^\lambda_{\lambda 2} + \Gamma^\lambda_{\lambda \sigma} \Gamma^\sigma_{22} - \Gamma^\lambda_{\sigma 2} \Gamma^\sigma_{\lambda 2} \\
&= \partial_1 \Gamma^1_{22} - \partial_2 \Gamma^3_{32} + \Gamma^\lambda_{\lambda 1} \Gamma^1_{22} - \Gamma^0_{\sigma 2} \Gamma^\sigma_{02} - \Gamma^1_{\sigma 2} \Gamma^\sigma_{12} - \Gamma^2_{\sigma 2} \Gamma^\sigma_{22} - \Gamma^3_{\sigma 2} \Gamma^\sigma_{32} \\
&= \partial_1 \Gamma^1_{22} - \partial_2 \Gamma^3_{32} + \Gamma^0_{01} \Gamma^1_{22} + \Gamma^1_{11} \Gamma^1_{22} + \Gamma^2_{21} \Gamma^1_{22} + \Gamma^3_{31} \Gamma^1_{22} - \Gamma^1_{22} \Gamma^2_{12} - \Gamma^2_{12} \Gamma^1_{22} - \Gamma^3_{32} \Gamma^3_{32} \\
&= \partial_1 \Gamma^1_{22} - \partial_2 \Gamma^3_{32} + \Gamma^0_{01} \Gamma^1_{22} + \Gamma^1_{11} \Gamma^1_{22} + \Gamma^3_{31} \Gamma^1_{22} - \Gamma^2_{12} \Gamma^1_{22} - \Gamma^3_{32} \Gamma^3_{32} \\
&= \frac{\partial}{\partial r}(-re^{-\lambda}) - \frac{\partial}{\partial \theta}(\cot \theta) + \frac{1}{2}\nu'(-re^{-\lambda}) + \frac{1}{2}\lambda'(-re^{-\lambda}) \\
&\quad + \frac{1}{r}(-re^{-\lambda}) - \frac{1}{r}(-re^{-\lambda}) - \cot^2 \theta \\
&= 1 - e^{-\lambda}\left(1 + \frac{1}{2}r(\nu' - \lambda')\right),
\end{aligned}
$$

$$
\begin{aligned}
R_{33} &= \partial_\lambda \Gamma^\lambda_{33} - \partial_3 \Gamma^\lambda_{\lambda 3} + \Gamma^\lambda_{\lambda \sigma} \Gamma^\sigma_{33} - \Gamma^\lambda_{\sigma 3} \Gamma^\sigma_{\lambda 3} \\
&= \partial_1 \Gamma^1_{33} + \partial_2 \Gamma^2_{33} + \Gamma^\lambda_{\lambda 1} \Gamma^1_{33} + \Gamma^\lambda_{\lambda 2} \Gamma^2_{33} - \Gamma^0_{\sigma 3} \Gamma^\sigma_{03} - \Gamma^1_{\sigma 3} \Gamma^\sigma_{13} - \Gamma^2_{\sigma 3} \Gamma^\sigma_{23} - \Gamma^3_{\sigma 3} \Gamma^\sigma_{33} \\
&= \partial_1 \Gamma^1_{33} + \partial_2 \Gamma^2_{33} + \Gamma^0_{01} \Gamma^1_{33} + \Gamma^1_{11} \Gamma^1_{33} + \Gamma^2_{21} \Gamma^1_{33} + \Gamma^3_{31} \Gamma^1_{33} + \Gamma^3_{32} \Gamma^2_{33} - \Gamma^1_{33} \Gamma^3_{13} \\
&\quad - \Gamma^2_{33} \Gamma^3_{23} - \Gamma^3_{13} \Gamma^1_{33} - \Gamma^3_{23} \Gamma^2_{33} \\
&= \partial_1 \Gamma^1_{33} + \partial_2 \Gamma^2_{33} + \Gamma^0_{01} \Gamma^1_{33} + \Gamma^1_{11} \Gamma^1_{33} + \Gamma^2_{21} \Gamma^1_{33} - \Gamma^1_{33} \Gamma^3_{13} - \Gamma^3_{23} \Gamma^2_{33} \\
&= \frac{\partial}{\partial r}\left(-re^{-\lambda} \sin^2 \theta\right) + \frac{\partial}{\partial \theta}(-\sin \theta \cos \theta) + \frac{1}{2}\nu'(-re^{-\lambda} \sin^2 \theta) \\
&\quad + \frac{1}{2}\lambda'(-re^{-\lambda} \sin^2 \theta) + \frac{1}{r}(-re^{-\lambda} \sin^2 \theta) - \frac{1}{r}(-re^{-\lambda} \sin^2 \theta) \\
&\quad - \cot \theta(-\sin \theta \cos \theta) \\
&= \sin^2 \theta \left[1 - e^{-\lambda}\left(1 + \frac{1}{2}r(\nu' - \lambda')\right)\right] \\
&= R_{22} \sin^2 \theta.
\end{aligned}
$$

Summarizing we have that the only non zero Ricci's tensor components are

$$
R_{00} = \left(\frac{1}{2}\nu'' + \frac{1}{4}\nu'^2 - \frac{1}{4}\nu'\lambda' + \frac{\nu'}{r} \right) e^{\nu - \lambda},
$$

$$
R_{11} = -\frac{1}{2}\nu'' + \frac{1}{4}\nu'\lambda' - \frac{1}{4}\nu'^2 + \frac{\lambda'}{r},
$$

$$
R_{22} = 1 - e^{-\lambda} \left(1 + \frac{1}{2}r(\nu' - \lambda') \right),
$$

$$
R_{33} = R_{22} \sin^2 \theta.
$$

1.3 Curvature scalar

The also known as Ricci's scalar for the metric (2.8) is calculated as follows

$$
\begin{aligned}
R &= g^{\mu\nu} R_{\mu\nu} = R^\mu_\mu \\
&= g^{00} R_{00} + g^{11} R_{11} + g^{22} R_{22} + g^{33} R_{33} \\
&= g^{00} R_{00} + g^{11} R_{11} + g^{22} R_{22} + g^{33} R_{22} \sin^2 \theta \\
&= g^{00} R_{00} + g^{11} R_{11} + (g^{22} + g^{33} \sin^2 \theta) R_{22} \\
&= e^{-\lambda} \left(\frac{1}{2}\nu'' + \frac{1}{4}\nu'^2 - \frac{1}{4}\nu'\lambda' + \frac{\nu'}{r} \right) - e^{-\lambda} \left(-\frac{\nu''}{2} - \frac{1}{4}\nu'^2 + \frac{1}{4}\nu'\lambda' + \frac{\lambda'}{r} \right) \\
&\quad - \frac{2}{r^2} \left(1 - e^{-\lambda} \left(1 + \frac{1}{2}r(\nu' - \lambda') \right) \right) \\
&= e^{-\lambda} \left(\nu'' + \frac{1}{2}\nu'^2 - \frac{1}{2}\lambda'\nu' + \frac{2}{r}(\nu' - \lambda') + \frac{2}{r^2} - \frac{2}{r^2}e^{\lambda} \right).
\end{aligned}
$$

1.4 Einstein's tensor components

Once the scalar and the Ricci components have been calculated, it is possible to calculate the non-zero components of the Einstein tensor from Eq. (2.2), resulting in

$$
\begin{aligned}
G_{00} &= R_{00} - \frac{1}{2}Rg_{00} \\
&= e^{\nu-\lambda}\left(\frac{1}{2}\nu'' + \frac{1}{4}\nu'^2 - \frac{1}{4}\nu'\lambda' + \frac{\nu'}{r}\right) \\
&\quad -\frac{1}{2}e^{\nu-\lambda}\left(\nu'' + \frac{1}{2}\nu'^2 - \frac{1}{2}\lambda'\nu' + \frac{2}{r}(\nu'-\lambda') + \frac{2}{r^2} - \frac{2}{r^2}e^{\lambda}\right) \\
&= e^{\nu-\lambda}\left[\frac{\lambda'}{r} + \frac{1}{r^2}(e^{\lambda}-1)\right],
\end{aligned}
$$

$$
\begin{aligned}
G_{11} &= R_{11} - \frac{1}{2}R_{11} \\
&= -\frac{1}{2}\nu'' + \frac{1}{4}\nu'\lambda' - \frac{1}{4}\nu'^2 + \frac{\lambda'}{r} \\
&\quad +\frac{1}{2}\left(\nu'' + \frac{1}{2}\nu'^2 - \frac{1}{2}\lambda'\nu' + \frac{2}{r}(\nu'-\lambda') + \frac{2}{r^2} - \frac{2}{r^2}e^{\lambda}\right) \\
&= \frac{\nu'}{r} + \frac{1}{r^2} - \frac{e^{\lambda}}{r^2},
\end{aligned}
$$

$$
\begin{aligned}
G_{22} &= R_{22} - \frac{1}{2}Rg_{22} \\
&= 1 - e^{-\lambda}\left(1 + \frac{1}{2}r(\nu'-\lambda')\right) \\
&\quad +\frac{1}{2}r^2 e^{-\lambda}\left(\nu'' + \frac{1}{2}\nu'^2 - \frac{1}{2}\lambda'\nu' + \frac{2}{r}(\nu'-\lambda') + \frac{2}{r^2} - \frac{2}{r^2}e^{\lambda}\right) \\
&= \frac{1}{2}re^{-\lambda}(\nu'-\lambda') + \frac{1}{2}r^2 e^{-\lambda}\nu'' + \frac{1}{4}r^2\nu'^2 e^{-\lambda} - \frac{1}{4}r^2\lambda'\nu'e^{-\lambda} \\
&= \frac{1}{4}r^2 e^{-\lambda}\left(2\frac{\nu'-\lambda'}{r} + 2\nu'' - \lambda'\nu' + \nu'^2\right),
\end{aligned}
$$

$$G_{33} = R_{33} - \frac{1}{2}Rg_{33}$$

$$= R_{22}\sin^2\theta - \frac{1}{2}Rg_{33}$$

$$= R_{22}\sin^2\theta - \frac{1}{2}R(-r^2\sin^2\theta)$$

$$= \sin^2\theta\left(R_{22} - \frac{1}{2}R(-r^2)\right)$$

$$= \sin^2\theta\left(R_{22} - \frac{1}{2}Rg_{22}\right)$$

$$= G_{22}\sin^2\theta.$$

In summary, the only non null Einstein's tensor components for the metric (2.8) are

$$G_{00} = e^{\nu-\lambda}\left(\frac{\lambda'}{r} - \frac{1}{r^2} + \frac{1}{r^2}e^\lambda\right)$$

$$G_{11} = \frac{1}{r}\left(\nu' + \frac{1}{r}(1 - e^\lambda)\right)$$

$$G_{22} = \frac{1}{4}r^2 e^{-\lambda}\left(2\nu'' - \lambda'\nu' + \nu'^2 + 2\frac{\nu' - \lambda'}{r}\right)$$

$$G_{33} = G_{22}\sin^2\theta.$$

Annex B

Auxiliary functions I

$$\zeta = a_2 + a_3 r^2 \qquad \chi = \ln\left(1 + \frac{a_3}{a_2}r^2\right)$$

$$
\begin{aligned}
\eta_1 &= 6a_1 a_2^3 C^3 r^2 + a_2^2 a_3 C \left(3a_1 C r^2 \beta_2(r) + 8a_3^2\right) \\
&\quad + a_2 a_3^2 C r^2 \left(8a_3^2 - a_1 \left(C^2 r^4 + 6\beta_3(r)\right)\right) - 2a_1 a_3^3 r^2 \\
\eta_2 &= a_2^2 B \left(3a_3^2 - 2a_1 B r^2\right) - a_1 a_3^2 r^2 + a_2 a_3 B r^2 \left(3a_3^2 - a_1 \gamma_2(r)\right),
\end{aligned}
$$

$$
\begin{aligned}
\varrho_1 &= a_3 A \left(3a_2 + a_3 r^2\right) + a_2 B \left(a_2 - a_3 r^2\right) \\
\varrho_2 &= 8a_2 a_3^3 C^2 \left(C r^2 \beta_5(r) + 6\right) \zeta(r)^2 + a_1 \mathcal{S}_1(r) \\
\varrho_3 &= 3a_2 a_3^2 B^2 \left(B r^2 + 3\right) \zeta(r)^2 + a_1 \mathcal{S}_2(r)
\end{aligned}
$$

$$\mathcal{P}_1 = a_2 B^2 \left(5a_1 r^2 + 8a_3 \zeta(r)\right) - a_1 AB \left(a_2 - 5a_3 r^2\right) - a_1 a_3 A^2$$

$$\mathcal{P}_2 = 4a_1 a_3 ABr^2 \left(2a_2 + a_3 r^2\right)$$
$$+ a_2 B^2 \left(4a_2 r^2 \left(a_1 + 4a_3^2\right) + a_3 r^4 \left(a_1 + 8a_3^2\right) + 8a_2^2 a_3\right) - a_1 a_2 a_3 A^2$$

$$\mathcal{P}_3 = 6a_1 a_2 C\beta_8(r)(a_3 - a_2 C)^2 \zeta(r)\chi(r) + 8a_2 a_3^4 C\beta_1^3 \zeta(r)$$
$$+ a_3 \beta_8(r)\left[-6a_1 a_2^3 C^3 r^2 + a_2^2 a_3 C \left(-3a_1 Cr^2 \beta_9(r) - 8a_3^2\right)\right.$$
$$\left. + a_2 a_3^2 Cr^2 \left(a_1 \left(Cr^2 \beta_{10}(r) - 6\right) - 8a_3^2\right) + 2a_1 a_3^3 r^2 \right],$$

$$\mathcal{P}_4 = -18a_1 a_2 C^2 (a_3 - a_2 C)^2 \zeta(r)^2 \chi(r)$$
$$+ 24a_2 a_3^4 C^2 \chi(r)^2 + 6a_2^2 a_3^2 C^2 r^2 \left(Cr^2 \beta_7(r) + 3\right)$$
$$+ a_1 a_3 \left[18a_2^4 C^4 r^2 + 9a_2^3 a_3 C^3 r^2 \left(3Cr^2 - 4\right)\right.$$
$$\left. - a_2 a_3^3 \left(8C^4 r^8 + 34C^3 r^6 + 14Cr^2 + 1\right) - 6a_3^4 Cr^4 \right]$$

$$\mathcal{P}_5 = a_3 r^2 \left[a_1 \gamma_6(r) \left(2a_2^2 B^2 + a_2 a_3 B\gamma_2(r) + a_3^2\right) + 3a_2 a_3^2 B^2 \gamma_7(r)\zeta(r) \right]$$
$$- 2a_1 a_2 B\gamma_6(r)(a_2 B - a_3)\zeta(r)\chi(r)$$

$$\mathcal{P}_6 = 15a_2 a_3^3 B^2 \zeta(r)^2 + 10a_1 a_2 B^2 (a_2 B - a_3)\zeta(r)^2 \chi(r)$$
$$+ a_1 a_3 \left[-10a_2^3 B^3 r^2 + 5a_2^2 a_3 B^2 r^2 \gamma_8(r) - 5a_3^3 Br^4 \right.$$
$$\left. + a_2 a_3^2 \left(Br^2 \left(-9B^2 r^4 + Br^2 - 11\right) - 1\right) \right],$$

$$\mathcal{S}_1 = 6a_2^4 C^3 \beta_4(r) + 3a_2^3 a_3 C^2 \left(3Cr^2 \beta_6(r) + 4\right)$$

$$+ 2a_2^2 a_3^2 C \beta_4(r) \left(Cr^2 \beta_7(r) + 3\right) - 2a_3^4 r^2 \beta_4(r)$$

$$+ a_2 a_3^3 \left(Cr^2 \left(Cr^2 \left(Cr^2 \beta_3(r) + 48\right) + 4\right) + 6\right)$$

$$\mathcal{S}_2 = -2a_2^3 B^2 \gamma_3(r) + a_2^2 a_3 B \left(Br^2 \gamma_4(r) - 2\right)$$

$$+ a_2 a_3^2 \left(Br^2 \left(Br^2 \gamma_5(r) + 3\right) + 3\right) - a_3^3 r^2 \gamma_3(r)$$

$$\beta_1 = Cr^2 + 1 \quad \beta_2 = Cr^2 - 4 \quad \beta_3 = Cr^2 - 1$$

$$\beta_4 = 3Cr^2 - 1 \quad \beta_5 = Cr^2 + 3 \quad \beta_6 = 3Cr^2 - 5$$

$$\beta_7 = Cr^2 - 9 \quad \beta_8 = 9Cr^2 + 1 \quad \beta_9 = Cr^2 - 4$$

$$\beta_{10} = Cr^2 + 6$$

$$\beta_{11} = -6a_2^3 C^3 - 3a_2^2 a_3 C^2 \beta_9 + 2a_3^3 + a_2 a_3^2 C \left(Cr^2 \beta_{10} - 6\right),$$

$$\gamma_1 = Br^2 + 1 \quad \gamma_2 = Br^2 - 2 \quad \gamma_3 = Br^2 - 1$$

$$\gamma_4 = 5 - 3Br^2 \quad \gamma_5 = Br^2 + 9 \quad \gamma_6 = 7Br^2 + 1$$

$$\gamma_7 = Br^2 - 5 \quad \gamma_8 = 2 - 3Br^2.$$

$$\gamma_9 = 2a_2^2 B^2 + a_2 a_3 B \gamma_2 + a_3^2.$$

Annex C

Auxiliary functions II

$$\zeta(r) = a_2 + a_3 r^2$$

$$\varrho(r) = A^2(3a_2 + a_3 r^2) + r^2(5a_2 + 3a_3 r^2)$$

$$\chi(r) = \ln\left(1 + \frac{a_3}{a_2}r^2\right)$$

$$\tau(r) = a_3 A\left(3a_2 + a_3 r^2\right) + a_2 B\left(a_2 - a_3 r^2\right)$$

$$\varsigma(\beta, x) = R^2\left(\beta + a_3 x^2\right)$$

$$\zeta(\beta, x) = a_2 + \beta x^2$$

$$\chi(\beta, x) = \ln\left(1 + \frac{\beta}{a_2}x^2\right)$$

$$\mathcal{P}_1(\alpha, \beta, x) = 3R^6\bigg(a_3^2\alpha^2 x^2\left(1 - x^2\right) + \beta a_3\left(3\alpha^2 + 3x^4 - \left(\alpha^2 + 1\right)x^2\right)$$

$$+\beta^2\left(2\alpha^2 + 5x^2 - 3\right)\bigg)$$

$$\mathcal{P}_2(\alpha, \beta, x) = R^4\left(\beta\left(2\alpha^2 + 3x^2 - 3\right) - a_3\alpha^2\left(x^2 - 3\right)\right)$$

$$\mathcal{P}_1(r) = 6A^2 a_2^2 - 3R^2 \left(a_2 - A^2 a_3\right)\left(3a_2 + a_3 r^2\right)$$
$$-3A^2 a_3 r^2 \zeta(r) + 15a_2^2 r^2 + 9a_2 a_3 r^4$$

$$\mathcal{P}_2(r) = A^2 \left(2a_2 - a_3 r^2 + 3a_3 R^2\right) + 3a_2(r - R)(r + R)$$

$$\mathcal{P}_3(r) = a_2 B^2 \left(5a_1 r^2 + 8a_3 \zeta(r)\right) - A^2 a_1 a_3 - a_1 AB \left(a_2 - 5a_3 r^2\right)$$

$$\mathcal{P}_4(r) = -\left(9Cr^2 + 1\right)\left(6a_1 a_2 C(a_3 - a_2 C)^2 \zeta(r)\chi(r) + a_3 \eta_3(r)\right)$$
$$-8a_2 a_3^4 C \left(Cr^2 + 1\right)^3 \zeta(r)$$

$$\mathcal{P}_5(r) = 6a_2^4 C^3 \left(3Cr^2 + 1\right) - 2a_3^4 r^2 \left(3Cr^2 + 1\right)$$
$$-3a_2^3 a_3 C^2 \left(-9C^2 r^4 + 9Cr^2 + 4\right)$$
$$+2a_2^2 a_3^2 C \left(C^2 r^4 \left(3Cr^2 - 26\right) + 3\right)$$
$$+a_2 a_3^3 Cr^2 \left(Cr^2 \left(Cr^2 \left(7Cr^2 + 13\right) + 48\right) + 16\right)$$

$$\vartheta_1(\alpha, \beta, x) = \alpha a_2 \zeta(\beta, x)^2 \chi(\beta, x)$$
$$-\beta x^2 \left(a_2 \beta \left(3A - \alpha x^2\right) + A\beta^2 x^2 + \alpha a_2^2\right)$$

$$\vartheta_2(\alpha, \beta, x) = \beta(\beta A + \alpha a_2) - \alpha a_2(a_2 + \beta)\chi(\beta, x)$$

$$\vartheta_3(\alpha, \beta, x) = (5\alpha - A)\left(A - \alpha x^2\right)$$

$$\vartheta_4(\alpha, \beta, x) = x^2(5\alpha - A)\ln(a_2 + \beta) + \left(A - 5\alpha x^2\right)\ln\zeta(\beta, x)$$
$$+A\left(x^2 - 1\right)\ln(a_2)$$

$$\vartheta_5(\alpha, \beta, x) = \alpha a_2 \zeta(\beta, x)^2 \chi(\beta, x) - \beta x^2 \left(A\beta^2 x^2 + \alpha a_2^2 + 4\alpha a_2 \beta x^2\right)$$

$$\vartheta_6(\alpha, \beta, x) = \beta(\beta A + \alpha a_2) - \alpha a_2(a_2 + \beta)\ln\left(1 + \frac{\beta}{a_2}\right)$$

$$\vartheta_7(\alpha, \beta, x) = \beta x^2(\beta A + \alpha a_2) - \alpha a_2 \zeta(\beta, x)\chi(\beta, x).$$

$$\eta_1(r) = 6a_1a_2^3C^3r^2 + a_2^2a_3C\left(3a_1Cr^2\left(Cr^2 - 4\right) + 8a_3^2\right)$$

$$+a_2a_3^2Cr^2\left(8a_3^2 - a_1\left(C^2r^4 + 6Cr^2 - 6\right)\right) - 2a_1a_3^3r^2$$

$$\eta_2(r) = 8a_2a_3^3C^2\left(Cr^2\left(Cr^2 + 3\right) + 6\right)\zeta(r)^2$$

$$+a_1\Bigg(6a_2^4C^3\left(3Cr^2 - 1\right) + 2a_3^4r^2\left(1 - 3Cr^2\right)$$

$$+2a_2^2a_3^2C\left(3Cr^2 - 1\right)\left(Cr^2\left(Cr^2 - 9\right) + 3\right)$$

$$+3a_2^3a_3C^2\left(3Cr^2\left(3Cr^2 - 5\right) + 4\right)$$

$$+a_2a_3^3\Big(Cr^2\left(Cr^2\left(Cr^2\left(Cr^2 - 1\right) + 48\right) + 4\right) + 6\Big)\Bigg)$$

$$\eta_3(r) = a_2^2a_3C\left(-3a_1Cr^2\left(Cr^2 - 4\right) - 8a_3^2\right)$$

$$+a_2a_3^2Cr^2\left(a_1\left(Cr^2\left(Cr^2 + 6\right) - 6\right) - 8a_3^2\right)$$

$$+2a_1a_3^3r^2 - 6a_1a_2^3C^3r^2$$

$$\eta_4(r) = 3a_3Cr^2(2a_3 - a_2C) - 6(a_3 - a_2C)^2 + a_3^2C^2r^4$$

$$\eta_5(r) = 6a_2C(a_3 - a_2C)^2\zeta(R)\chi(R)$$

$$+a_3R^2\Bigg(-6a_2^3C^3 - 3a_2^2a_3C^2\left(CR^2 - 4\right)$$

$$+a_2a_3^2C\left(CR^2\left(CR^2 + 6\right) - 6\right) + 2a_3^3\Bigg)$$

$$\varrho_1(\alpha, \beta, x) = 6\alpha^3a_2^4\left(3\alpha x^2 - 1\right) + 3\alpha^2a_2^3\beta\left(3\alpha x^2\left(3\alpha x^2 - 5\right) + 4\right)$$

$$+2\alpha a_2^2\beta^2\left(3\alpha x^2 - 1\right)\left(\alpha x^2\left(\alpha x^2 - 9\right) + 3\right)$$

$$+a_2\beta^3\Bigg(\alpha x^2\Big(\alpha x^2\left(\alpha x^2\left(\alpha x^2 - 1\right) + 48\right) + 4\Big) + 6\Bigg)$$

$$+2\beta^4x^2\left(1 - 3\alpha x^2\right)$$

$$\varrho_2(\alpha, \beta, x) = \beta\Bigg(6\alpha^3a_2^3 + 3(\alpha - 4)\alpha^2a_2^2\beta - (\alpha(\alpha + 6) - 6)\alpha a_2\beta^2 - 2\beta^3\Bigg)$$

$$-6\alpha a_2(a_2 + \beta)(\beta - \alpha a_2)^2\ln\left(1 + \frac{\beta}{a_2}\right)$$

$$\varrho_3(\alpha, \beta, x) = (\alpha(\alpha + 3) - 6)(a_2 + \beta)(\beta - \alpha a_2)^2$$

$$\varrho_4(\alpha, \beta, x) = 6\alpha a_2(a_2 + \beta)(\beta - \alpha a_2)^2 \zeta(\beta, x)\varrho_6(\alpha, \beta, x) - \beta\varrho_5(\alpha, \beta, x)$$

$$\varrho_5(\alpha, \beta, x) = -6\alpha^3 a_2^4 \left(\alpha\left((\alpha(\alpha + 3) - 6)x^2 + 9\right) + 1\right)$$
$$-3\alpha^2 a_2^3 \beta\varrho_7(\alpha, \beta, x) + \alpha a_2^2 \beta^2 \varrho_8(\alpha, \beta, x)$$
$$+2(\alpha + 1)^3 \beta^4 x^2 + a_2 \beta^3 \varrho_9(\alpha, \beta, x)$$

$$\varrho_6(\alpha, \beta, x) = (\alpha + 1)^3 \ln(a_2) - (9\alpha + 1)\ln(a_2 + \beta) - \alpha(\alpha(\alpha + 3) - 6)\ln\zeta(\beta, x)$$

$$\varrho_7(\alpha, \beta, x) = \alpha\left(9\alpha + \alpha(\alpha(\alpha + 3) - 6)x^4 + 2\left(\alpha\left(\alpha^2 + \alpha - 3\right) + 13\right)x^2 - 35\right) - 4$$

$$\varrho_8(\alpha, \beta, x) = \alpha\left(\alpha(9\alpha + 55) + \alpha^2(\alpha(\alpha + 3) - 6)x^6 - 3(\alpha - 2)\alpha(\alpha(\alpha + 3) - 6)x^4\right.$$
$$\left.+3\left(\alpha\left(4\alpha^2 + \alpha + 5\right) + 16\right)x^2 - 48\right) - 6$$

$$\varrho_9(\alpha, \beta, x) = \alpha\left(x^2\left(\alpha\varrho_{14}(\alpha, \beta, x) - 18\right) + 18\right) + 2$$

$$\varrho_{10}(\alpha, \beta, x) = 6\alpha^3 a_2^4\left(3\alpha x^2 + 1\right) + 3\alpha^2 a_2^3 \beta\left(3\alpha x^2 - 4\right)\left(3\alpha x^2 + 1\right)$$
$$+2\alpha a_2^2 \beta^2\left(\alpha^2 x^4\left(3\alpha x^2 - 26\right) + 3\right) - 2\beta^4 x^2\left(3\alpha x^2 + 1\right)$$
$$+\alpha a_2 \beta^3 x^2\left(\alpha x^2\left(\alpha x^2\left(7\alpha x^2 + 13\right) + 48\right) + 16\right)$$

$$\varrho_{11}(\alpha, \beta, x) = 6\alpha a_2 \varrho_3(\alpha, \beta, x)\zeta(\beta, x)\chi(\beta, x) - x^2\varrho_{12}(\alpha, \beta, x)$$

$$\varrho_{12}(\alpha, \beta, x) = 2(6 - \alpha(\alpha + 3))\beta^4(a_2 + \beta)$$
$$-\alpha a_2 \beta(6 - \alpha(\alpha + 3))(a_2 + \beta)\varrho_{13}(\alpha, \beta, x)$$
$$-(9\alpha + 1)\left(\alpha x^2 + 2\right)\zeta(\beta, x)\varrho_2(\alpha, \beta, x)$$

$$\varrho_{13}(\alpha, \beta, x) = 6(\beta - \alpha a_2)^2 + 3\alpha\beta(\alpha a_2 - 2\beta)x^2 - \alpha^2 \beta^2 x^4$$

$$\varrho_{14}(\alpha, \beta, x) = \alpha(\alpha(\alpha + 3) - 6)x^2\left(\alpha x^2 + 6\right) + 3\alpha(\alpha + 13) - 6$$

$$\varphi_1(r) = a_2^2 B \left(3a_3^2 - 2a_1 B r^2\right) + a_2 a_3 B r^2 \left(a_1 \left(2 - B r^2\right) + 3a_3^2\right)$$
$$- a_1 a_3^2 r^2$$

$$\varphi_2(r) = a_1 \Bigg(-2a_2^3 B^2 \left(B r^2 - 1\right) + a_2^2 a_3 B \left(B r^2 \left(5 - 3B r^2\right) - 2\right)$$
$$+ a_2 a_3^2 \left(B r^2 \left(B r^2 \left(B r^2 + 9\right) + 3\right) + 3\right) + a_3^3 r^2 \left(1 - B r^2\right) \Bigg)$$
$$+ 3a_2 a_3^2 B^2 \left(B r^2 + 3\right) \zeta(r)^2$$

$$\varphi_3(r) = a_1 \left(7B r^2 + 1\right) \left(2a_2^2 B^2 + a_2 a_3 B \left(B r^2 - 2\right) + a_3^2\right)$$
$$+ 3a_2 a_3^2 B^2 \left(B r^2 - 5\right) \zeta(r)$$

$$\varphi_4(r) = a_2^2 a_3 B \left(-6B^2 r^4 + B r^2 + 2\right) - 2a_2^3 B^2 \left(2B r^2 + 1\right)$$
$$+ 2a_2 a_3^2 B r^2 \left(B r^2 \left(B r^2 + 6\right) + 3\right) - a_3^3 r^2 \left(2B r^2 + 1\right)$$

$$\varphi_5(r) = a_3 R^2 \left(2a_2^2 B^2 + a_2 a_3 B \left(B R^2 - 2\right) + a_3^2\right)$$
$$- 2a_2 B (a_2 B - a_3) \zeta(R) \chi(R)$$

$$\Upsilon(\alpha, \beta, x) = \frac{2\alpha a_2 \left(\alpha a_2 - \beta\right) \gamma_3(\alpha, \beta, x) \chi(\beta, x)}{(7\alpha + 1) \gamma_2(\alpha, \beta, x) x^2}$$

$$\gamma_1(\alpha, \beta, x) = \alpha a_2^2 \beta \left(\alpha x^2 \left(5 - 3\alpha x^2\right) - 2\right)$$
$$+ a_2 \beta^2 \left(\alpha x^2 \left(\alpha x^2 \left(\alpha x^2 + 9\right) + 3\right) + 3\right)$$
$$+ \beta^3 x^2 \left(1 - \alpha x^2\right) - 2\alpha^2 a_2^3 \left(\alpha x^2 - 1\right)$$

$$\gamma_2(\alpha, \beta, x) = \beta \left(2\alpha^2 a_2^2 + (\alpha - 2)\alpha a_2 \beta + \beta^2\right)$$
$$- 2\alpha a_2 (a_2 + \beta)(\alpha a_2 - \beta) \ln \left(1 + \frac{\beta}{a_2}\right)$$

$$\gamma_3(\alpha, \beta, x) = (\alpha - 5) (a_2 + \beta)$$

$$\gamma_4(\alpha, \beta, x) = 2\alpha^2 a_2^2 + \alpha a_2 \beta \left(\alpha x^2 - 2\right) + \beta^2$$

$$\gamma_5(\alpha, \beta, x) = \alpha a_2^2 \beta \left(-6\alpha^2 x^4 + \alpha x^2 + 2\right) + 2\alpha a_2 \beta^2 x^2 \left(\alpha x^2 \left(\alpha x^2 + 6\right) + 3\right)$$
$$- \beta^3 x^2 \left(2\alpha x^2 + 1\right) - 2\alpha^2 a_2^3 \left(2\alpha x^2 + 1\right)$$